AFRL-RV-PS-
TR-2019-0131

CALIBRATION OF SEISMIC LOCATION IN CENTRAL ANDES OF BOLIVIA

Gonzalo A. Fernandez M, et al.

Observatorio San Calixto
Calle Indaburo No. 944
PO Box 12656
La Paz, Bolivia

07 June 2019

Final Report

AIR FORCE RESEARCH LABORATORY
Space Vehicles Directorate
3550 Aberdeen Ave SE
AIR FORCE MATERIEL COMMAND
KIRTLAND AIR FORCE BASE, NM 87117-5776

DTIC COPY

NOTICE AND SIGNATURE PAGE

AFRL-RV-PS-TR-2019-0131 HAS BEEN REVIEWED AND IS APPROVED FOR PUBLICATION IN ACCORDANCE WITH ASSIGNED DISTRIBUTION STATEMENT.

//SIGNED//	//SIGNED//
Dr. Frederick Schult Program Manager, AFRL/RVB	Dr. Thomas R. Caudill, Chief AFRL Geospace Technologies Division

REPORT DOCUMENTATION PAGE

Form Approved
OMB No. 0704-0188

1. REPORT DATE *(DD-MM-YYYY)*	**2. REPORT TYPE**	**3. DATES COVERED** *(From - To)*
07-06-2019	Final Report	20 May 2016 – 31 May 2019

4. TITLE AND SUBTITLE

Calibration of Seismic Location in Central Andes of Bolivia

5a. CONTRACT NUMBER
FA9453-16-C-0045

5b. GRANT NUMBER

5c. PROGRAM ELEMENT NUMBER
DoD - DTRA

6. AUTHOR(S)

Gonzalo A. Fernandez M, Marcelo Assumpcao, Mayra Nieto, and Teddy Griffiths

5d. PROJECT NUMBER
DoD - DTRA

5e. TASK NUMBER
PPM00026935

5f. WORK UNIT NUMBER
EF129463

7. PERFORMING ORGANIZATION NAME(S) AND ADDRESS(ES)
Observatorio San Calixto
Calle Indaburo No. 944
PO Box 12656
La Paz, Bolivia

8. PERFORMING ORGANIZATION REPORT NUMBER

9. SPONSORING / MONITORING AGENCY NAME(S) AND ADDRESS(ES)
Air Force Research Laboratory
Space Vehicles Directorate
3550 Aberdeen Avenue SE
Kirtland AFB, NM 87117-5776

10. SPONSOR/MONITOR'S ACRONYM(S)
AFRL/RVBN

11. SPONSOR/MONITOR'S REPORT NUMBER(S)
AFRL-RV-PS-TR-2019-0131

12. DISTRIBUTION / AVAILABILITY STATEMENT
Approved for public release; distribution is unlimited (AFMC-2019-0676 dtd 15 Nov 2019)

13. SUPPLEMENTARY NOTES

14. ABSTRACT
The Central Andes is a high plateau with elevations above 3400 m., the crustal thickness and shortening process due to the subduction between the Nazca and South America plates, the seismicity along the Central Andes is distributed by sources, the crustal shallow seismicity is related to natural crust deformation, especially on the Bolivian Orocline (from), depths are distributed from 5 to 70 km. Subduction processes have two sources, intermediate from 100 to 350 km depth and deeper from 500 to 650 km. Furthermore far away seismicity also affects the Central Andes. Locating earthquakes in the region is always difficult, with a lot of uncertainty due to Moho variations along the Central Andes. Further there was not enough data to perform tomography to resolve the problem. After 2016 a 1D velocity model based on the previous research on receiver functions in the Central Andes was proposed and the results showed more coherency and accuracy also with international agencies. Different location algorithms were tested with our 1D velocity model which showed better performance, especially when we applied iLOC 3D locating software. Once earthquakes were accurate located, we proposed to obtain focal mechanism solutions to enhance the knowledge of seismicity for the Central Andes. The method applied was the double couple with first polarities of waveforms. Each result has at least one plane coherent with the geologic context. Furthermore with the data already processed a Moment Tensor Inversion was calculated for three seismic events, those events showed coherent results that helped us to understand the fault procedure.

15. SUBJECT TERMS
Central Andes, earthquake location, focal mechanism

16. SECURITY CLASSIFICATION OF:			**17. LIMITATION OF ABSTRACT**	**18. NUMBER OF PAGES**	**19a. NAME OF RESPONSIBLE PERSON**
a. REPORT	**b. ABSTRACT**	**c. THIS PAGE**			Dr. Frederick Schult
Unclassified	Unclassified	Unclassified	Unlimited	58	**19b. TELEPHONE NUMBER** *(include area code)*

This page is intentionally left blank.

Table of Contents

List of Figures

List of Tables

ACKNOWLEDGEMENT

We would like to thank the Air Force Research Laboratory (AFRL – FA9453-16–C–0045) for support during the period of the research. Also to Jorge Roman-Nieves and George Mirda for the constant reviews of our reports. Without them this work would not have been possible to do. To Jamie Ryan and Susan Beck from University of Arizona for giving us the data to work with. To Marcelo Assumpcao from Sao Paulo University for the constant spread of knowledge to our team.

This page is intentionally left blank.

1. SUMMARY

The present work has focused on relocating crustal shallow earthquakes from 2011 to 2015. There was a no accurate velocity model however until 2016 after studies on crustal thickness made it possible to elaborate a 1D velocity model for the Western Cordillera, Altiplano and Eastern Cordillera. After that a relocating procedure was performed and eight earthquakes were analyzed to obtain the fault plane solutions and if possible the moment tensor inversion. Three of them had coherent solutions and accurate seismic parameters.

2. INTRODUCTION

The Central Andes is an example of the mountain building process that is associated with the subduction between Nazca and South America plates along the forearc. As a consequence a shortening process it is observed as the principal contributing factor for the development of the thick crust and high elevation at Central Andes (Beck et al., 1996; Myers et al., 1998; Ward et al., 2013).

Five major morphological /structural subparallel units divide the Central Andes, from West to East, the Western Cordillera with high mountains, 2) the Altiplano a flat plateau, 3) the Eastern Cordillera composed of high altitude mountains dominated by folding and thrusting of Paleozoic and Cenozoic rocks, 4) the Inter Andean zone and then 5) the Sub Andes which has an active thin – skinned fold and thrust belt (Beck et al., 1996; Eichelberger, 2015). Moreover the Central Andes show significant changes related to crustal thickness, the Western and Eastern Cordillera reach approximately 70km thick, the Altiplano goes to around 60 km, East and the Craton are at 35 km (Beck and Zandt, 2002; Ryan et al., 2016).

Due to lateral variations in the Wadatti – Benioff zone caused by the descending high velocity slab location errors are often introduced, sometimes fewer if the depth is less than 50km, but for deeper earthquakes (subduction) the error can be higher. Furthermore Bolivian seismicity is distributed via seismogenic sources based on depth, the first one belongs to shallow source crustal earthquakes with depths than 70km; next are subduction earthquakes with depths between 100 to 350 km and finally, deep earthquakes with depths from 500 to 650 km. There are also distant sources, which are earthquakes originating in Southern Peru and Northern Chile.

Recent studies of the Central Andes, in collaboration with Arizona University under Project CAUGHT / PULSE (Central Andes Uplift High Topography / Peru Lithosphere and Slab Experiment) showed tomography models for the region. Ward et al. (2013) applied Ambient Noise Tomography (ANT) to obtain high resolution maps in the crust and uppermost mantle based on vertically polarized shear wave velocity (V_{sv})

derived from high – quality Rayleigh wave dispersion. Ryan et al. (2016) applied the Receiver Function method (RF) to attain the structure of the crust in the Bolivian Orocline of the Central Andes in northern of Bolivia and Southern Peru.

Ward et al. (2013) and Ryan et al. (2016) results were taken into account as inputs in order to refine a better velocity model for the Western Cordillera, Altiplano, and Eastern Cordillera. To improve the regional velocity model two algorithms were applied, a Joint Hypocenter Determination (JHD) and iLOC, a 3D location method proposed by Bondar and Storchak (2011).

Once the velocity model was calibrated, a set of crustal shallow earthquakes were re picked and re located using crustal phases, the Ground Truth (GT) quality controls were applied for the final list of data that were proposed for further analysis related to the fault plane solutions and, in some cases, a moment tensor inversion.

Finally, we present a list of ten earthquakes that show enhanced accuracy in terms of locations, geological context, and stress regime. Those eight events have clear first P(g/n) wave polarity. Analysis was conducted using different methodologies such as FOCMEC by Snoke (2003) and Moment Tensor Inversion by Dreger (2000). The solutions obtained during the project were added to the national focal mechanism database to provide a better knowledge of the crustal shallow seismicity and an improvement to seismic hazard analysis.

3. TECHNICAL APPROACH

3.1. Tectonic Setting and Seismogenic Sources in Bolivia.

The Central Andes covers a broad land mass area from 12°S to 42°S and defines the typical example of an active Cordillera-type orogeny with tectonics associated with subduction of the oceanic Nazca Plate under the continental South American plate and increased westward drift of the South American Plate as an important driving tectonic shortening mechanism in the Cenozoic era.

Moreover, along strike variations in the geometry of the East–dipping subducting Nazca slab have resulted in different styles of crustal deformation associated with segments of flat – slab subduction. This phenomenon is also associated with volcanic cessation which defines the Central Volcanic Zone (CVZ) of the Central Andes.

The rate of shifting (estimated) between Nazca and South America plates is from 58 mm/year to 80 mm/year. Also there is a similar rate of 15 mm/year distributed over a broad zone of deformation located at Central Andean Cordillera.

This shortening process is also evident where the Andean orogen is widest, with active deformation over 800km inland from the trench (Ward et al. 2013). Below the Central Andes, the dip of the Nazca slab shallows shortens to ~ 50°, two segments of very shallow slab border the Central Andes, but at depths greater than 200km the slab bends again into dips of 70 – 80 ° (Eichelberger et al. 2016).

The Central Andes retroarc has been effectively divided into five tectonomorphic zones defined by major steps in mean topographic and structural elevations. From West to East, the Western Cordillera (WC) is a high, active volcanic arc with peaks reaching 6000 m., then bordered to the East by the Altiplano (AP). The AP is a high elevation, low – relief plateau with an average altitude of about 3800 m. Next is the Eastern Cordillera (EC), a high mountain range dominated by folding and thrusting of Paleozoic through Cenozoic rocks. Further East is the Inter Andean (IA), a narrow transitional zone of intermediate structural and topographic levels between the Eastern Cordillera and the Sub Andes. The Sub Andean zone (SA) is an active thin – skinned fold and thrust belt. Finally the Chaco and Beni Plain basin is a stable platform underlaid by the Brazilian Craton (Beck et al. 1996; Ward et al. 2013; Ryan et al. 2016).

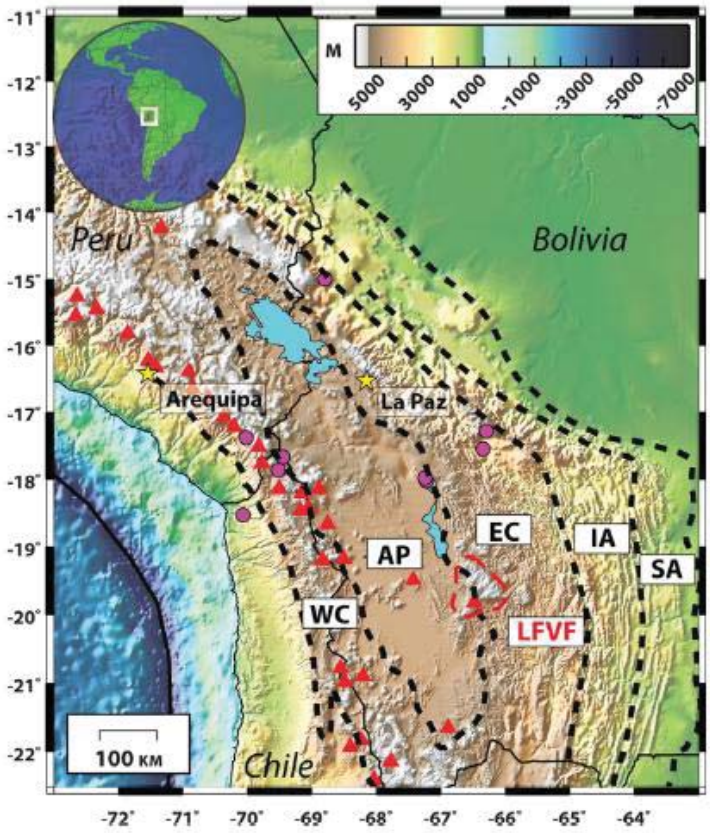

Figure 1. Central Andes tectonomorphic zones delimitations.

The exact age of the deformation and uplift of the Altiplano, Western Cordillera, and Eastern Cordillera is not tightly constrained, but previous studies agree that the uplift occurred in the past 27 million years (Scire et al. 2015). Crustal shortening in the Central Andes, about 300 km total, has occurred since 45 Ma, but 1 – 3 km uplift of the Eastern Cordillera also occurred with little upper crustal shortening in the last 10 – 15 Ma (Leier et al. 2013; Ryan et al. 2016).

Ryan et al. (2016) summarizes the various proposed mechanisms for the rapid EC uplift in the last 10Ma, which include isostatic compensation from both deep processes (delaminations) and surface processes, such as climate induced erosion. A complete understanding of the crustal evolution and current geodynamic processes requires comprehensive mapping of the present crustal stresses in the Central Andes.

The seismogenic sources in the Central Andes are divided into three categories, the first source is related to crustal deformation and a shortening process, the second is related to the subduction process, and the third is related to distant sources.

a. *The Seismogenic Sources Related to Crustal Deformation:* The first seismogenic sources in the Crust related to the continental deformation have seismic events with depths less than 75Km. This depth applies to the Bolivian crustal thickness. It is associated with areas that have continental deformation, The spatial locations in the crust allow us to define two sub – sources.

i. The first sub – source is related to potentially active faults that have generated seismicity, probably in the Holocene age (quaternary period). Evidence of this can be seen at the surface and can be identified due to the geologic features, geomorphologic and structural present in the current sediments.

ii. The second sub – source is related to seismicity in distinct crustal plates which have a depth greater than five kilometers. These kinds of events occur around the Cochabamba region and are induced by the convergence of the Nazca Plate and South America Plate along the forearc.

b. *Seismogenic Sources Related to Subduction Processes*: Earthquakes from this seismogenic source are located inside the Nazca Plate. They originate due to the subduction process where the upper part of the slab presents an interplate coupling zone defined by a change in the compressional tension stress field. There are two sub sources for these kinds of events.

i. Between 100 to 350 Km: Known as an intermediate earthquake, the occurrence frequency is greater than the subduction earthquakes. They can be found around the La Paz (south west), Oruro, and Potosi regions.

ii. Between 500 to 700Km: Known as deep earthquakes. The main characteristic is that they do not occur all the time, however, they can generate magnitudes higher than 7 Mw. As an example, the earthquake of 09-06-1994, a 8 Mw Magnitude, was located under La Paz (North), Santa Cruz, and Tarija regions.

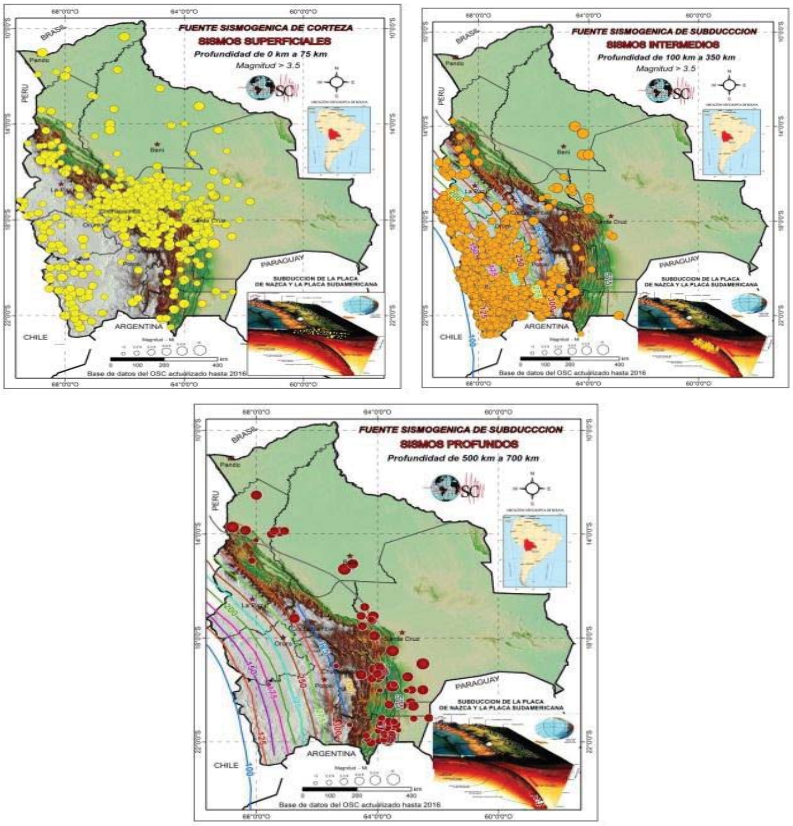

Figure 2 Seismogenic sources for Bolivia. *Yellow dots represent shallow, crustal seismicity. Orange dots represent the subduction seismicity depth between 100 to 350 km. Red dots indicate subduction earthquakes with depths between 500 to 650 km.*

3.2. Ground Truth Definition and Applications.

The main objective of the presented research is to apply a "Ground Truth" methodology to improve seismic location in the Central Andes. But what does "Ground Truth" mean?.

"Seismic reference events" were originally based on international catalogs such as ISC, NEIC and local country catalogs. For an earthquake to be considered a "seismic reference event", it needed to have an error ellipse between 10 to 15km and more than 50 P phases picked.

Bondar and Storchak (2011) introduced the nomenclature of "Ground Truth" categories like Gtx, where x is the epicenter location accuracy in km. They proposed a selection criteria based on network geometry to assess the location accuracy of seismic events. As an example he stated that a GT5 candidate must have a 95% confidence level and at least ten seismic station arrivals within 250km as well as an azimuthal gap of less than 110° with a secondary azimuthal gap of less than 160°. Finally at least one station should be within 35 km of the epicenter.

Later Bondar modified the selection criteria, so that all stations must be within 150 km, second, the azimuthal gap should be less than 160°, and at least one station should be within 10 km of the epicenter and the quality metric of less than 0.35 (for more information related to the quality metric refer to "A new ground truth dataset for seismic studies". Bondar & McLaughlin 2009).

However Bondar & McLaughlin (2009) has elevated demands for small seismic networks and a well constrained velocity model. To try to extend the applications Boomer et al.(2010) proposed to apply statistical methods such as the Jacknife or Bootstrap. The principle idea was to reduce location uncertainty by resampling the data (Bootstrap) and subsequently estimate the location through iterative steps until a statistic of interest was achieved (Jacknife) providing empirical probability distributions for the statistics.

Both authors assumed at the very least that the research center has a dense seismic network installed (can be permanent or temporary) with well constrained azimuthal coverage. If no such network existed, the statistical methods would not provide extra support to the analysis.

Others have proposed keeping the relative location methods within a cluster of events using arrival – time differences between pairs of stations, using a well – constrained master event and follow-on comparisons of nearby events with similar waveforms.

That technique allows us to apply it to homogenous and heterogeneous isotropic and anisotropic media. Grid search and travel time interpolation would be independent for any velocity model, 1D or 3D. This is a versatile procedure for locating seismic events and can be applied to different kinds of surface models without modifying the grid search itself.

Deichman & Garcia – Fernandez (1992) applied the relative location techniques to improve the final result on seismic clusters over the State of California. After the time and onset corrections, location software such as HypoDD , JHD, or a 3D method were applied to refine final locations with more accuracy than the initial solution.

The IASPEI Commission on Seismic Observation and Interpretation (CoSOI) working group on Reference Events for Improved Locations coordinated the search and worked with different seismological centers like the ISC (International Seismological Centre) and CTBTO (The Comprehensive Nuclear-Test-Ban Treaty Organization) to store and distribute the GT seismic event results.

Storchark et al. (2015) integrated the ISC and CTBTO database in order to search for more GT events and to take into account other methodologies than Bondar and McLaughlin (2009). INSAR (Interferometric Synthetic – Aperture Radar) and relative locations were added to the methodology proposed before.

A near final concept of GT events was presented as one or a group of seismic events that fulfill the selection criteria proposed by Bondar and McLaughlin (2009) relative to location accuracy and taking into account different methodologies like relative locations and INSAR before computing a final solution (Storchark et al. 2015). Nonetheless, the final location methodology is open, which means that the seismological center can use any method described above, including the velocity model which can be one or three dimensional.

Lienert & Havskov (1995) modified the Hypocenter algorithm to obtain a flexible tool to locate local, regional and teleseismic earthquakes that works with the NORDIC format inside the SEISAN earthquake location software. The NORDIC format enables running the Hypocenter algorithm for the same or multiple earthquakes multiple times.

Hypocenter is an iterative earthquake location program that works with an adaptive – damped least squares method, which allows running hypocentral corrections many times, searching for the potential minimum root mean square (rms). However, accuracy of the velocity model is fundamental to obtain coherent rms results in order to reach a near absolute seismic event location (Lienert & Havskov 1995).

There are advantages to using the Lienert & Havskov (1995) Hypocenter algorithm modification, the initial travel time consistency is performed by selection of the type of earthquake. The algorithm proposed using L for “Local”, R for “Regional” and T for “Teleseismic”. Moreover, the program allows applying an initial location based on fast –picking P and S phases and then, in combination with IASPEI travel times, a suggested

phase is printed, although the analyst's expertise will define the final phase (Leinert & Havskov, 1995).

Ultimately, this algorithm allows us to acquire hypocentral corrections based on weighting the least–squares inversion. This means, instead of calculating an origin time correction, the algorithm centers the residuals to improve numerical stability to depth solutions. This allows the r.m.s to increase temporarily for a set of iterations to search for a potential lower minimum. If the search is successful then we have the final depth result (Leinert & Havskov, 1995).

As mentioned before, the absolute location done by the Leinert & Havskov (1995) Hypocenter modification algorithm is not the final word. Some bias may be encountered as the depth of the phases picked can increase the error and ambiguity of the solution. This ambiguity can increase if we have a set of earthquakes from the same region (an earthquake cluster), then the final results will not align to the potential fault plane.

The Joint Hypocenter Determination (JHD) is used to improve relative earthquake locations and quantify lateral structural variations. This method was introduced into a sub – routine in 2000 within SEISAN software.

The main goal of the JHD technique is to determine errors due to the over – simplified velocity model of earth structure. Errors can result near the hypocenter, the stations, or the ray path propagation. To treat these kinds of errors, a station time correction can be accomplished disregarding irregularities near the earthquake hypocenters. Two steps are taken into account. The first determines the station correction based on origin time and hypocenter. The second one takes the results of the first step and performs a least squares inversion to redo the calculation and finally applies the same technique as the modified Hypocenter by Leinert & Havskov (1995), so the lowest value on r.m.s will be the final result.

The final result done by the JHD technique can be applied on the algorithm VELEST in order to get an improved velocity model versus the first one proposed. In other words, VELEST and JHD work together to improve the absolute location based on relative locations.

Nowadays, a 1D velocity model is not enough to validate absolute location. If we assume that it is the final one, the tendency guides us to apply 3D velocity models obtained from seismic tomography or receiver functions. Solutions proposed by Myers et al. (2010) allow the researcher to apply a 3D model to refine/ relocate their earthquakes using the Regional Seismic Travel Time (RSTT) technique. However, it is not accurate for regions with low seismicity and/or with insufficient information due to

a lack of seismic stations. Likewise, RSTT was elaborated for North America and European regions. This issue makes it difficult to apply outside of the areas mentioned before (Myers et al., 2010).

iLOC is a 3D location model based on the RSTT technique that can be integrated into the Seiscomp3 database. Basically, iLOC (ISC Locator) works seamlessly with AK135 and RSTT phases (crustal and depth), once the data has been picked. The Neighborhood Algorithm also known as "NA" obtains the initial hypocenter, then linearized inversions are applied to estimate a covariance matrix to account for correlated model errors (Bondar & McLaughlin 2009).

The depth will be fixed, if the region is not well constrained, yet most of the time the region is well constrained from previous studies. Later, a depth – phase estimate based on reported surface reflections via depth – phase stacking is calculated. Finally network magnitude is calculated with some level of uncertainty.

One iLOC advantage, in comparison with other 3D earthquake locators, is that one can set up its own 1D velocity model, so that the crustal phases will have more accuracy and a more precise depth will be produced.

3.3. Velocity Model Studies and Proposal for the Central Andes.

One of the main parameters for calculating earthquake location is understanding the velocity model in the region of interest. The accuracy of the velocity model (velocity vs depth) will allow us to better interpret seismic behavior (Housen et al 2010).

It is well known the Central Andes is the largest orogenic plateau in the world associated with abundant arc volcanism. It is also known that there are multiple segments of flat – slab subduction zones making this part of the Earth a unique place to study various aspects of active plate tectonics (Ward et al. 2013). The subduction process and crustal shortening force researchers make it so that a coherent and accurate velocity model is necessary to improve earthquake locations (Ward et al. 2013).

From 2010 to 2012, an extensive, temporarily – deployed seismic network (50 broadband stations) were emplaced in the Central Andes. These projects were conducted by the University of Arizona, these projects were called CAUGHT and PULSE (Central Andes Uplift and the Geodynamic of High Topography – Peru Lithospheric and Slab Experiment).

Within both projects, two techniques were proposed with a velocity model for the Central Andes to improve previous models proposed within the BANJO and SEDA

project (Broadband Andean Joint Experiment and Seismic Exploration of the Deep Altiplano) also conducted by University of Arizona on 1994 (Ward et al. 2013; Ryan et al. 2016).
Ward et al. (2013) proposed to initiate a continental – scale ambient noise tomography study with all data registered from the projects mentioned before. The primary goal was to vertically image polarized shear wave velocity (V_{sv}) structures of the South American Cordillera (Ward et al. 2013).

The use of dispersion measurements, calculated from cross–correlation data, led to the construction of Rayleigh wave phase velocity maps in the period range of 8 to 40 s and invert them to obtain the V_{sv} (Ward et al. 2013).

A dispersion misfit map and uncertainty envelopes for V_{sv} model were provided as a final result. It was possible to fully extend the technique until a mid – crust Andean low – velocity zone. With all results received, a phase velocity map was built with periods of 40 s. and the final 3D shear wave velocity (V_{sv}) model was constructed to model all tectonic settings of the Central Andes (Ward et al. 2013).

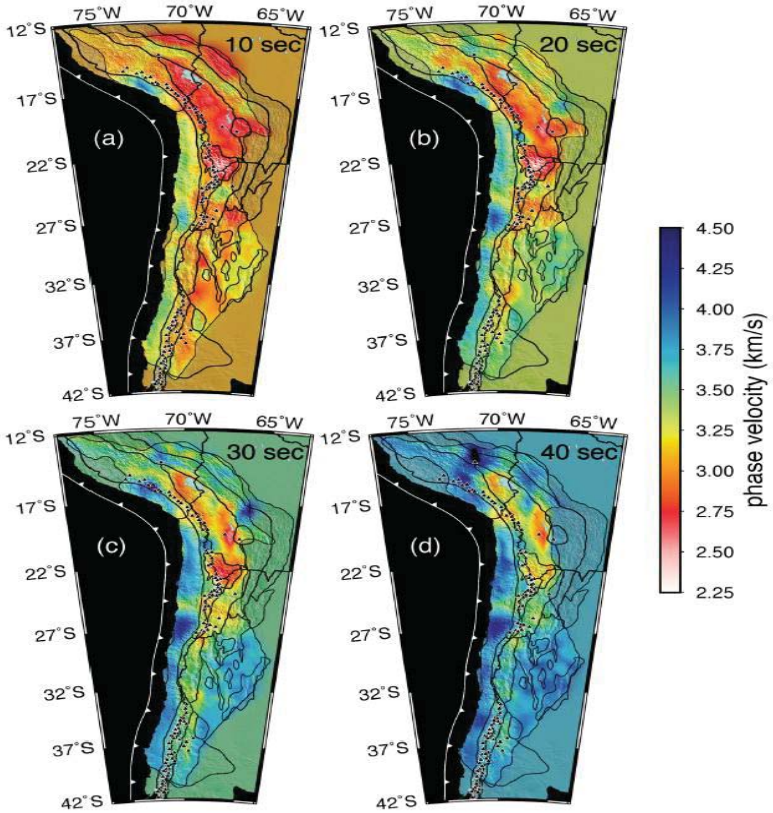

Figure 3. The 3D phase velocity map for the South America continent was done with Ambient Noise Tomography with data from CAUGHT / PULSE and BANJO / SEDA projects.

Ryan et al. (2016) proposed the Receiver Functions technique to model the crustal structure of the Central Andes. He also used data from the CAUGHT / PULSE and BANJO / SEDA projects. Results demonstrate the Receiver Functions provide a more detailed map of crustal thickness, improving the older maps from local studies.

Moreover, it was possible to model the volcanic arc utilizing Moho depths increasing from the Central Altiplano (65km) to the northern Altiplano (75km). The Eastern Cordillera displays large strike variations in crustal thickness. There is a small region of thin crust beneath the high peaks of the Cordillera Real where average elevations are near 4km and Moho depth varies between 55 to 60 km. At 20 degrees south, a deeper Moho is present (from 65 to 70 km depth). It appears that isostatic equilibrium occurs around this location (Ryan et al. 2016).

Several mid crustal discontinuities across the region were found and correlate well with known geology and improved the maps of Assumpcao et al. (2013) and Chulick et al. (2013). Moreover, the Eastern Cordillera has a low velocity region in the lower crust. This can be interpreted as melting, assimilation, storage and a homogenization process for the zone. Finally, the results show 3D Moho variations for the Central Andes. With this information, we were able to propose a 1D velocity model to work with during the research (Ryan et al. 2016).

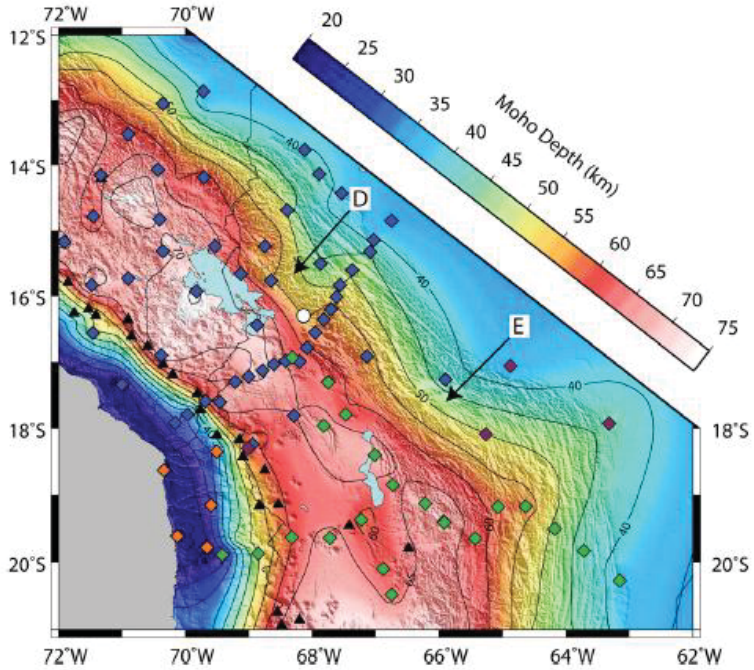

Figure 4. 3D Moho depth variations and velocity profile for the Central Andes. *Model proposed by Ryan et al. (2016).*

3.4. Focal Mechanics and the first motion of P waves.

In order to get the solution to the "Double – Couple" model we use the high – frequency approximation of geometrical optics, a most remarkable P wave property is the conservation of ana or kata seismic character along the entire seismic ray, all the way to a receiving seismic station at the Earth's surface where the anaseismic wave results in a initial upward motion of the ground. Meanwhile the kataseismic one gives a downward first motion. This is the most applied method since the 90's to get focal mechanics, which have a common representation as a beachball.

The focal mechanics can change in a mere solid rotation in space however does not change its nature, as this concept represent the high level of symmetry, the two planes defining the quadrants are conceptually interchangeable and, as a result, there exists an inherent indeterminacy between two possible physical solutions obtained from any field of seismic data generated by a point source, for example a left – lateral strike – slip earthquake on a vertical fault.

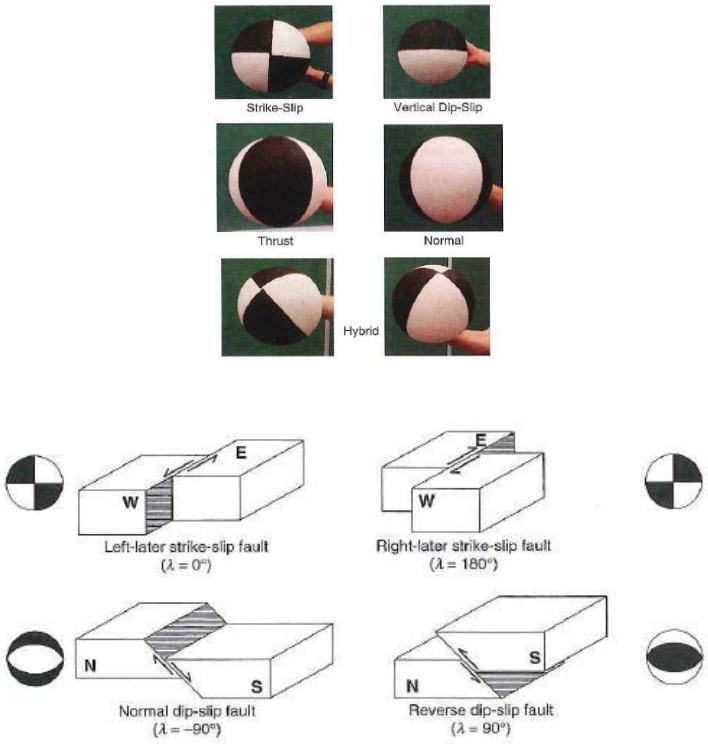

Figure 5. Beach ball representation for the different types of fractures.

3.5. Moment Tensor Inversion.

A representation of a seismic source using a symmetric tensor of the second order, generally clarifying that the entries are couples (dipoles) with different

orientations is called the Moment Tensor. Commonly it is interpreted upon its decomposition into subterms.

Minson and Dreger (2008) reviewed the moment tensor decomposition and confirmed that first there is an isotropic term that describes the amount of volumetric change at the seismic source. The other decomposition is called deviatoric which is unique but is subjective in nature.

Further decomposition related to the double couple (DC) can be described as shear faulting that identifies two candidate planes for the fault orientation. Then a compensated linear vector dipole (CLVD) model is present, which results in a net – volumetric source deformation. To model a tectonic earthquake it is recommended to calculate the decomposition as the sum of DC and CLVD.

Mathematically speaking, moment tensors are the product of scalar moments and normalization matrices. Scalar moment provides information about the released moment and the moment magnitude; this is often used to assess the average slip of the rupture area. The normalization matrix furnishes information about the rupture type, the rupture geometry, as well as the role of shear, tensile and isotropic components (Cesca and Heimann, 2016).

To resolve an earthquake source model: a moment tensor inversion (MTI) technique is needed. Practically, the MTI is a computation of synthetic seismograms for a given source model (moment tensor) and a given propagation between source and receivers (Green's Function). There are several methods available to perform the MTI. Several include first wave polarities, body waves amplitudes, amplitudes ratios, full waveforms, or amplitude spectra (Cesca and Heimann, 2016).

In this research, Dreger et al (2000) was used. The method proposed to evaluate a full waveform inversion for regional and local earthquakes. This methodology is based on an error fitting measure. Basically, both techniques assess the correlation and normalization to earthquake data and its synthetics to obtain absolute amplitude information.

Furthermore, error handling is minimized by applying the sum of the squared error and a process of iteration. The following equations show the error handling at the moment of the inversion. E is the error, i is the component, T is the length of the seismogram, $f_i(t)$ is the data vector, and $g_i(t)$ is the Green function vector.

$$E_i = 1 - \frac{\int_0^T |f_i(t) g_i(t)| dt}{\sqrt{\int_0^T f_i(t)^2 dt} \sqrt{\int_0^T g_i(t)^2 dt}} \quad (1)$$

$$E_i = \int_0^T [f_i(t) - g_i(t)^2] dt \quad (2)$$

As this method works with three component instrument data at varying distances, the moment tensor M_{ij} is a second rank symmetric tensor that describes a generalized system of forces at the seismic source. Moreover, it is usually decomposed into a series of different moment tensors. However, there is no unique decomposition, these are DC, CLVD, and isotropic terms (Dreger et al. 2000).

Dreger (2000) suggests to assess the goodness of fit, a variance estimate for each inversion is computed as:

$$\sigma = \sum_i \sum_j \sum_k \frac{(d_{ijk} - s_{ijk})^2}{N - M} \quad (3)$$

Where i, j, k are the station, component and time sample, d and s are the estimated and observed time series, N is the total number of points and M is the total number of free parameters. Results will depend whether we would desire to solve the DC, ISO + DC and Full MT (M = 5, 6 and 7 respectively). Therefore, the second fit is related to data normalization yielding a percent variance reduction – VR (Dreger et al., 2000).

$$VR = \left\{1 - \frac{\sum_i \sum_j \sum_k (d_{ijk} - s_{ijk})^2}{\sum_i \sum_j \sum_k (d_{ijk})^2}\right\} * 100 \quad (4)$$

The final equation is used to determine the optimal source depth, which is found through a grid search, for which the interval can be set within our seismological context.

4. RESULTS AND DISCUSSION

4.1. Data Selection and Velocity Model Validation.

As mentioned before, Bondar and McLaughlin (2009) proposed a new procedure to classify earthquakes according to epicenter location accuracy, network geometry and azimuthal gap. The, method is called Ground Truth (GT). Earthquakes that fulfill this criteria will be named GTx, where x is the accuracy of location.
A GT list is hosted by the ISC (International Seismological Centre). Earthquakes included on the list are also part of "Reference Events for Improved Locations" managed by the Commission on Seismic Observation and Interpretation (CoSOI).

The requirements to "categorize" a GTx event are difficult to achieve for a small seismic network with moderate, shallow activity. Moderate is defined as earthquakes

with magnitudes from 2.1 to 3.5 Mw. Statistical methods, such as the Jackknife or Bootstrap, were proposed by Boomer et al. (2010) to make some GTx events available in the seismic catalogs.

In the case of the Central Andes, we began compiling seismic catalogs available from the local Bolivian National Data Center (Observatorio San Calixto), then ISC, USGS, and the IDC. The period of time for all catalogs was from 2011 to 2015 as the first "time window". Due to a lack of sufficient seismic stations, it was decided to extend the time window through 2018 because since 2016, Observatorio San Calixto had installed 4 new broadband, 3 component seismic stations. This extension will be shown as tentative results for further analysis on annexes.

Table 1. List of seismic catalogs used within the research, organized by priority.

Catalog	Period Cover	Mc (Completeness Magnitude) – Type
OSC	2012-2018	3.3 Ml and Mw
ISC	2012-2015	4.0 Mw
USGS	2012-2018	4.0 Mw and mb
IDC	2012-2017	4.0 mb

Choosing a well constrained, coherent and accurate seismic catalog can be a challenge. Further, the objective of working with catalogs must be clear in order to attain proper results that can be related to seismic hazard, relocating seismic events, and/or quality control.

It is well known that each agency has their own algorithms to determine seismic locations. These formulas can be linear or nonlinear. The general velocity model can be used or, as indicated, a specific velocity model for the region (1D or 3D can be available). Seismic location calculation will never be absolute until a treatment procedure can be performed on the data. For example, relative locations with data from outside country borders or merging catalogs or adding your stations phase times can improve the final result.

In our scenario, we decided to work specifically with Central Andes shallow crustal earthquakes, most of them located on the Bolivian Orocline (near to 18° S). There were also various shallow crustal earthquakes used which were located in the Altiplano and Sub Andes region. During the period of interest (2012 – 2018), earthquakes with magnitude over 4 Mw occurred in those regions.

The majority of earthquakes reported in our seismic catalog are not included in the international agencies' catalogs due to low magnitudes. For that reason, in parallel with merging, our efforts were similar to the Advanced National Seismic System, Northern California Earthquake Data Center at UC Berkeley Seismological Laboratory (ANSS, NCEDC (2016). Using this procedure on dataset doi:10.7932/NCEDC), we were able to

comprehensively implement a waveform quality control procedure based on the work of Kishida et al.'s windowing method (2014).

Using the Kishida method, we were able to improve P and S picks and exclude seismograms that had signal to noise ratios (S.N.R.) lower than 30dB, due to their noisy characteristics and no clear arrival phases.

Moreover the azimuthal coverage was considered a quality control advantage displaying a consistent seismic station distribution, as mentioned in Bondar and McLaughlin (2009). To fulfill this objective we had to merge data from regional and temporary seismic networks around Bolivia.
Today, it is indispensable to work with data from other seismic networks because technology related to informatics has led us to utilizing open format data that can be analyzed in open source software too, such as SEISAN (Havskov J., Ottemoller L., Voss P., 2017). The seismic networks used during the research are the listed in Table 2.

Table 2. Seismic Stations and Networks used during the research, BB stands for Broadband and SP for short period.

Stations	Seismic Network	Time Window	Type of Installation	Type of sensors and components
LPAZ, BBOB, BBOD, BBOE, BBOE, SIV	GT and BO	2011 - 2018	Permanent	5 SP - Z, 5 BB – Z/NS/EO, 1 SP – Z/NS/EO
CAUGHT	ZG	2010 - 2012	Temporally	50 BB – Z/NS/EO
IPOC	CX	2011 - 2018	Permanent	20 BB – Z/NS/EO
Peru	--	2014	Permanent	4 BB – Z/NS/EO
Argentina	--	2014-2018	Permanent	1 SP – Z/NS/EO

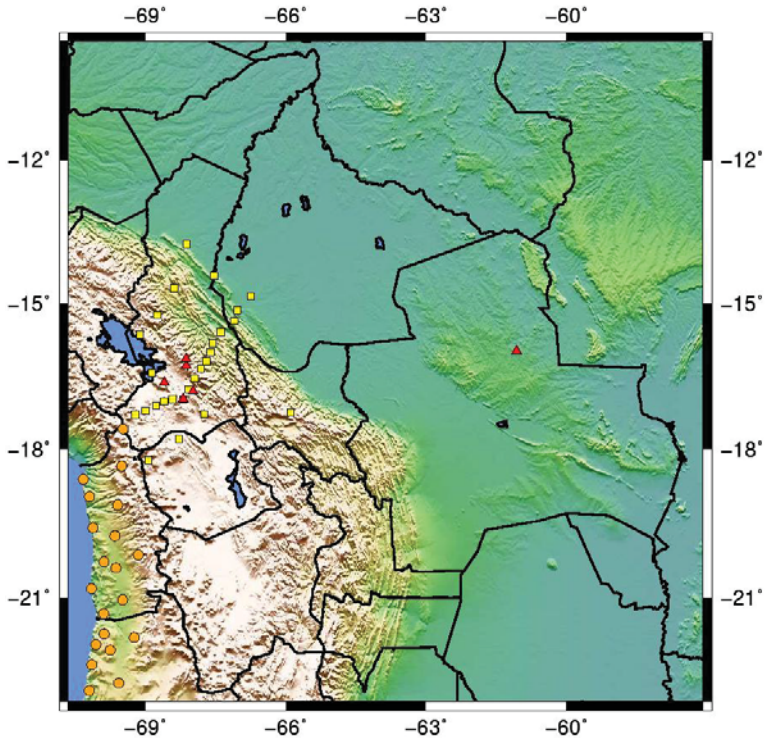

Figure 6. Seismic stations used for the research. *The red triangles represent permanent short period – one vertical component stations. Yellow squares represent CAUGHT broadband three components stations. Orange circles represent IPOC from Chilean seismic stations.*

The initial list of events is from 2012 to 2015. During this period, we took advantage of the CAUGHT data (Central Andes Uplift and Geographic High Topography), a dense linear seismic network installed in Bolivia from 2010 to 2012. Many shallow crustal earthquakes were recorded with at least 12 seismic stations.

After the 2012-2015 period, the local network was reduced to only 5 short period, single vertical component stations, 1 short period, three component instrument, and 1 broadband, three component sensor. Most of the stations are located in the Altiplano region, with just one station located in the Sub Andes region.

For that reason, we decided to integrate (or "incorporate") data from regional seismic networks such as the Chilean Integrated Plate Boundary Observatory Chile (IPOC)-CX seismic network. The distinct advantage of this coherent digital data is that we were able to successfully merge all waveforms together to calculate the seismic location.

Since 2016, 4 broadband, three component sensors were installed permanently around the Eastern Cordillera and Altiplano as a new seismic network named "RSOSC". Data integration was possible through application of Earthworm and SEISAN software tools (ISTI – Instrumental Software Technologies Inc.; Havskov J., Ottemoller L., Voss P.,

2017). Following the installation and incorporation of this software, seismic location procedures improved.

An example of data selected shows the seismic waveforms of an event which include data from the permanent, temporary, and regional seismic networks.

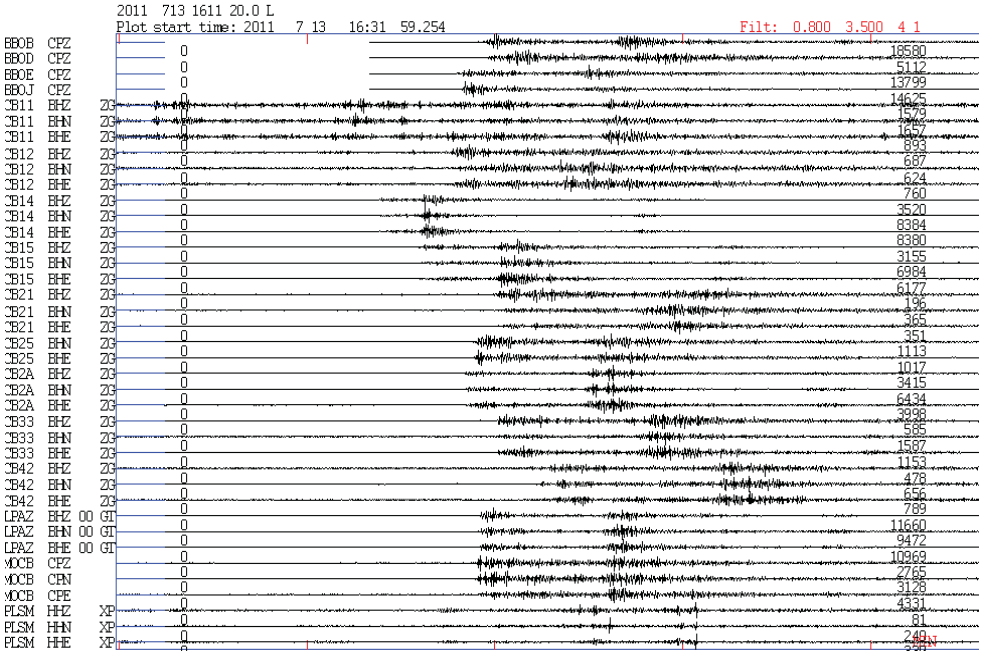

Figure 7. Local seismic event recorded by nearby permanent, temporary, and regional seismic stations. *Data are displayed in SEISAN.*

Despite Bondar and McLuaghlin's (2009) high level requirements to classify a seismic event inside the GTx list, especially for small seismic networks, we followed the azimuthal criteria and seismic station distribution approach. Moreover, waveform quality control using the Kishida et al. (2014) method was performed in order to comprehensively refine data to allow us to pick phases from the correct portion of the waveform.

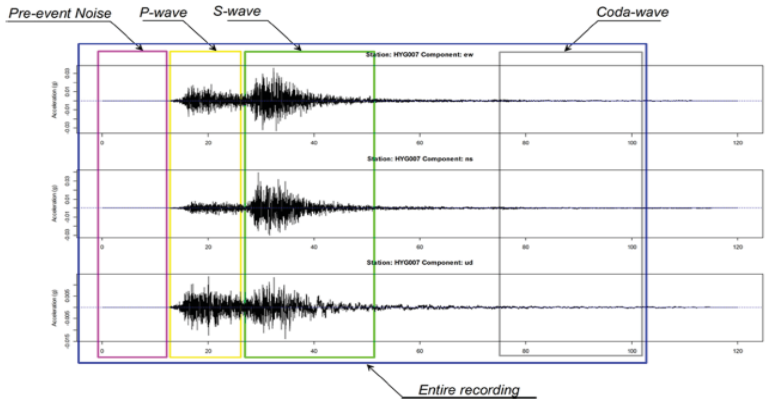

Figure 8. *Kishida et al. (2014)* Method to perform a quality control over the waveform in order to obtain at least 3 dB spectral separation between the data and noise.

The initial list was composed of 80 crustal shallow events. Following the application of quality control and merging of the catalogs according to ANSS methodology, which is similar to Bondar and McLaughlin (2009), we found that at least over one half of one percent of data should be removed. The main parameter to filter the initial catalog was through the use of the azimuthal gap and the number of seismic stations.

Moreover, depth and magnitude parameters were important to making a decision regarding the group of seismic events. Events with depths of 33 km are not well constrained due to the lack of a velocity model built for the Altiplano and Eastern Cordillera. As a result, most of the events were also removed from the initial list.

Until 2016, the Observatorio San Calixto calculated and completed daily analysis routines using a velocity model proposed by Minaya et al. (2012) which was based on previous tomography works such as the BANJO / SEDA project in collaboration with the University of Arizona. However, the velocity model was only calibrated for the middle areas of the Altiplano region roughly defined as 15.70°S to 16°S.

Most of the uncertainties related to this seismic location method are caused by measurement errors and by the unfavorable geometry of seismic stations that recorded the earthquake. The combinations of two components leads to scatter in the earthquake locations.

If velocity model errors are added to previous uncertainties many discrepancies result in conflict with international agencies' catalogs. Velocity model errors can be mitigated assuming some a priori knowledge of the maximum slowness perturbation.

For some crustal shallow earthquakes, located in the Eastern Cordillera or Sub Andes, we observed at least a 20km difference with the location from international agencies and sometimes the depth needed to be constrained to 15km to 33km. Solving it by computing the probability density function has been suggested, and NonLinLoc software was developed to do so, however it demands at least 10 seismic stations near the epicenter to be moderately effective.

Ryan et al. (2016) applied the Receiver Functions method to obtain the Moho depth under the Central Andes. Adding the application to his results was used as an input to get the new 1D velocity model for the Western Cordillera, Altiplano, and Eastern Cordillera.

One of our objectives was to approximate the 3D velocity model by a 1D model for Hypocenter. We did so through trial and error tests, relocating the earthquakes and comparing them with the international catalogs' locations. Following several trials, we found a useful and coherent model for the regions mentioned before.

Table 3. Velocity model obtained from Ryan et al. (2016) after the trial and error tests.

P Wave Velocity (km/s)	Depth (km)
5.5	0
6.2	10
8.2	60
8.2	65
8.5	80

Through expert analysis, we began to repetitively test the velocity model and the uncertainty range was reduced from 10km to 2 or 3 km. Moreover, the new seismic locations were near to geological faults that were studied in the past. This improvement led us to relocate the initial list. To do so we used the Joint Hypocenter Determination and VELEST algorithms in order to improve the velocity model and to obtain the P and S time corrections.

Having the P and S corrections helped to attain higher accuracy in depth resolution. Furthermore, we could start incorporating crustal phases such as $P_{g/n}$, $S_{g/n}$, L_g into the event solutions Using these seismic phases, the earthquake locations on the Altiplano and Eastern Cordillera also improved the error ellipses, reducing them down to almost 2 km. Each cross on the following figures represents a seismic station that was used to pick P and/or S phases to arrive at a final velocity model.

We ran the VELEST algorithm five times in combination with JHD with the idea to reduce the time residual to a lower value with each iteration. Moreover, JHD searched for best fit of depth and VELTEST for the best fit of times. This combination led us to the final velocity model.

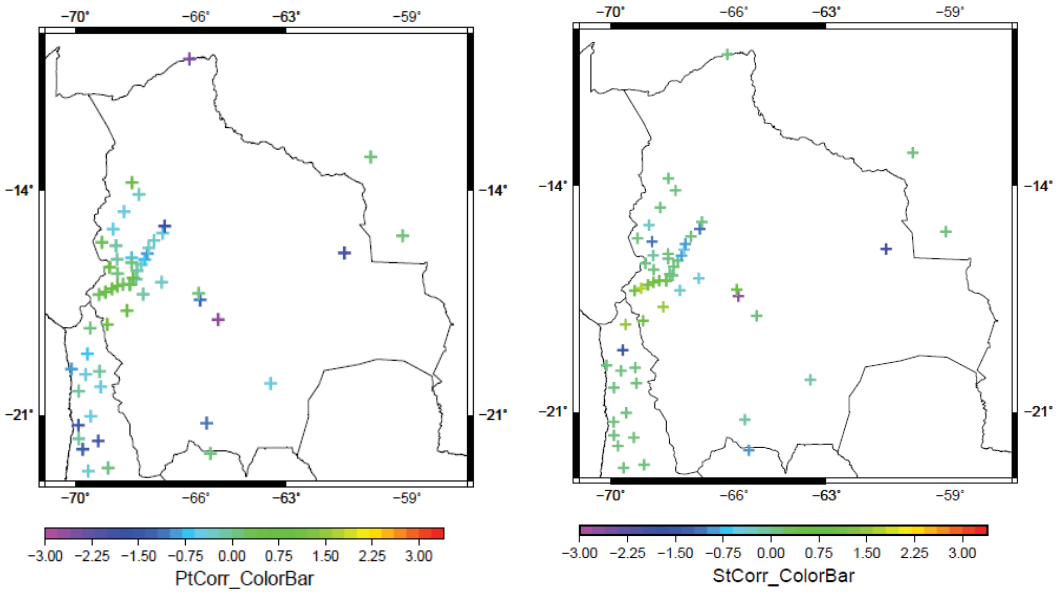

Figure 9. (Left) P time corrections for all seismic stations installed from 2010 to 2012. (Right) S time correction for the same period of time.

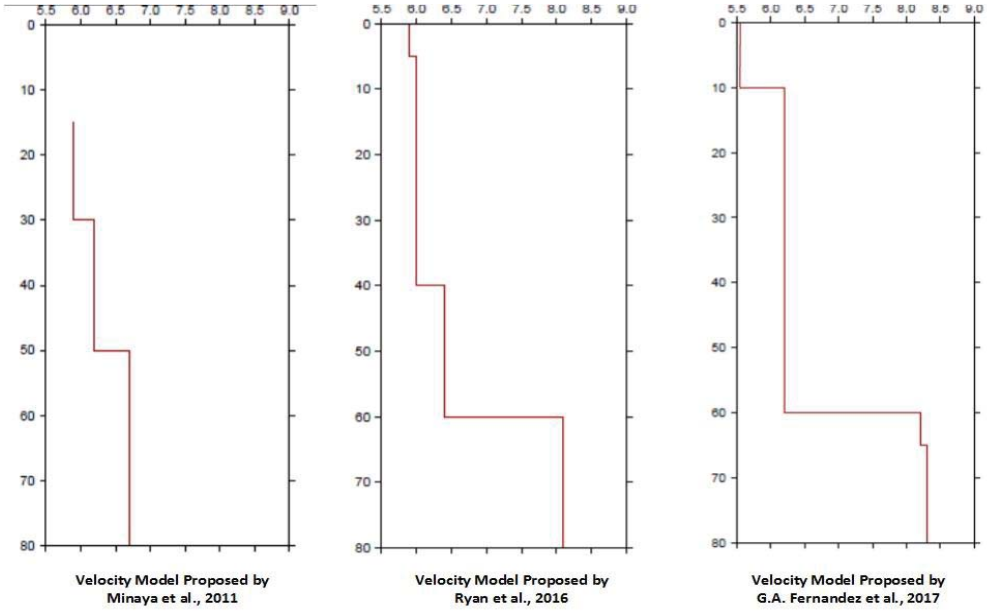

Figure 10. Velocity model enhancements. *JHD and VELEST algorithms led us to optimize results to more accurately determine the seismic location.*

Table 4. Final Velocity model obtained from Ryan et al. (2016) after JHD and VELTES algorithms applications.

Number of Iterations	5
Lowest Gap – Bigger Gap	99 – 331
Gap Average	193
Difference on Origin Time (dot) Absolute Adjustment	0.074
Final Vp velocity profile (Vp [km/s] Depth [km])	5.497 0.000 6.157 10.000 8.213 60.000 8.315 65.000 8.536 80.000
Final Vs velocity profile (Vp [km/s] Depth [km])	3.168 0.000 3.482 10.000 4.655 60.000 4.685 65.000 4.850 80.000
RMS average	0,1699

As shown on the previous figures, using the new velocity model in 1D we were able to determine $P_{(g/n)}$ and $S_{(g/n)}$ time shifts.

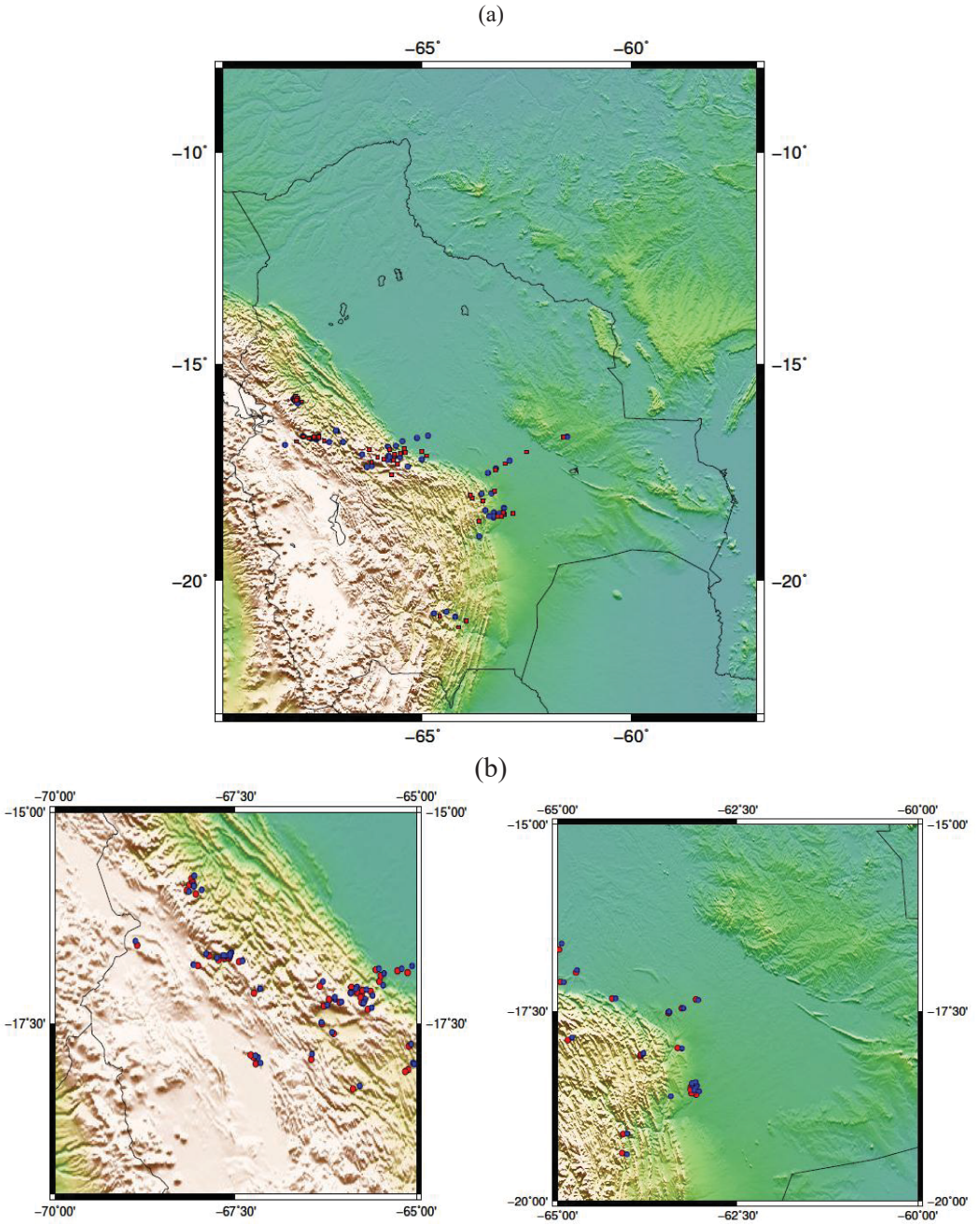

Figure 11. (a) Red points represent initial locations using the older velocity model. Blue points represent the new location with the new 1D velocity model, (b) A zoom of seismic events that were relocated.

We clearly noted seismic location improved, however we were not closer to fulfilling the Bondar and McLaughlin (2009) criteria. For that reason, we thought to validate each earthquake location with 3D location software for better accuracy on depth and seismic phase times.

The question may arise as to "what is the need to perform a seismic relocation in a 3D model again?", the answers are:

- Using a 3D velocity model profile, the travel-time predictions do not suffer from baseline differences between P, S and PKP phases compared to the Jeffreys –Bullen tables (Bondar and Storchak, 2011).
- A covariance matrix helps to assume the similarity between ray paths, so the P phases can be grouped by pairs. It will depend on the density of the network in the same or similar region. For example, the Altiplano is a region where a seismic station is installed, so the covariance matrix will allow pairs for the data.
- Bondar and Storchak (2011) with iLOC 3D location software has a process for calculating the depth, which helps to refine the crustal and depth phases.
- There is an option to specify a 1D velocity model in order to extrapolate and create a simulation of 3D velocity models for the desired region (Bondar and McLaughlin, 2009).

We used the iLOC 3D software in order to corroborate the location and the depth as well as the seismic phases. Another advantage was that the ellipse error, the azimuthal gap, and the back azimuth computation were easily calculated. We applied Bondar and McLaughlin (2009) azimuth criteria (less than 110°) to start the selection of seismic events that would be candidates for further analysis.

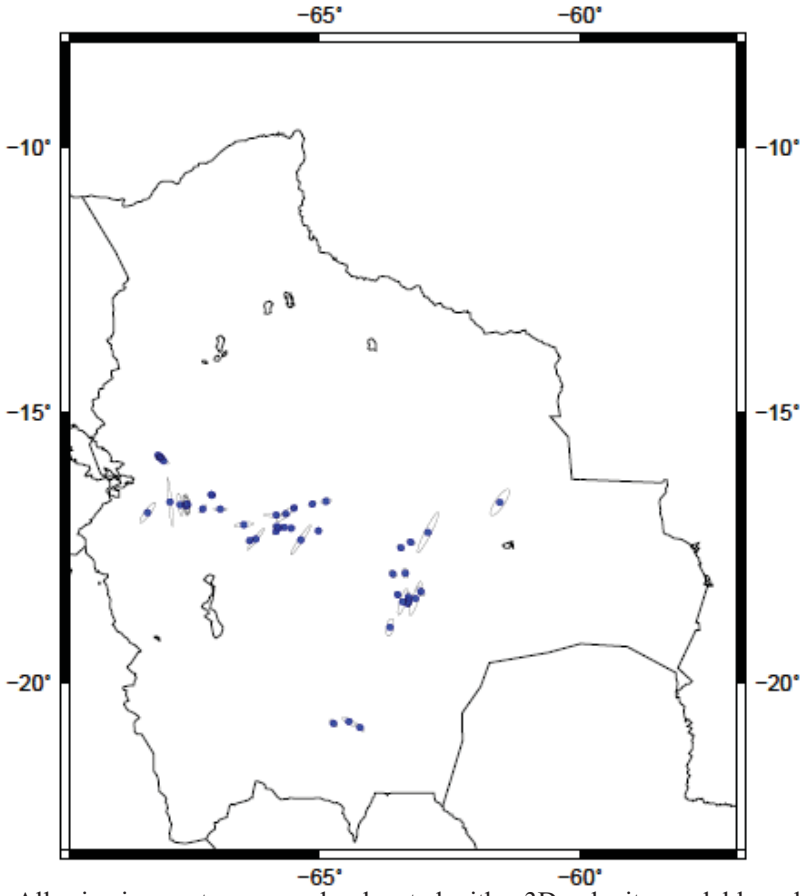

Figure 12. All seismic events proposed, relocated with a 3D velocity model based on our 1D model. Each ellipse represents the error.

If the ellipse error exceeds 10 km, then the seismic event is not accurate enough to perform further analysis such as focal mechanism or moment tensor inversion due to being poorly constrained in depth and location. We worked with events that had error ellipses lower than 12 km and the travel times tables fitted with phase picks. As an example, we will show a seismic event that was rejected and another that was accepted.

(a)

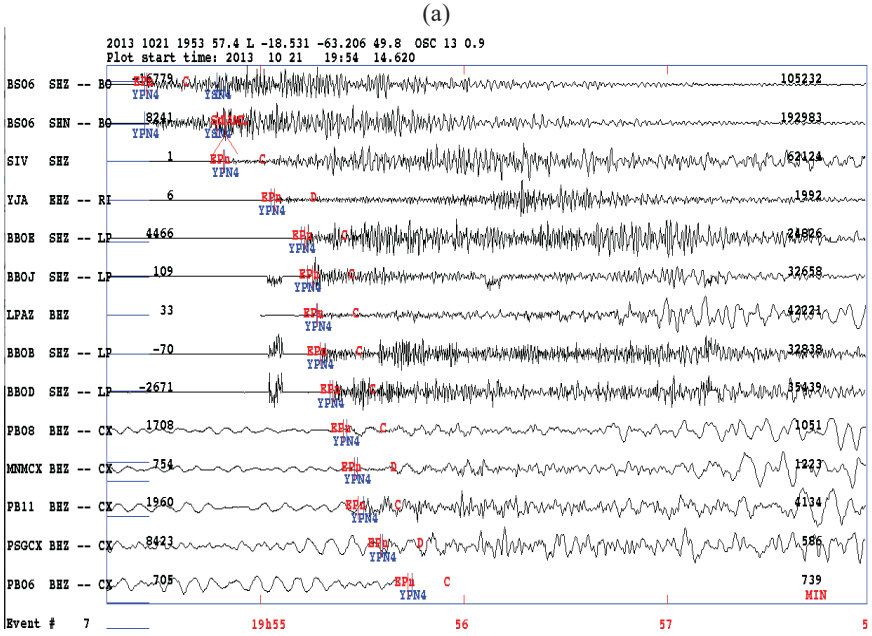

(b)

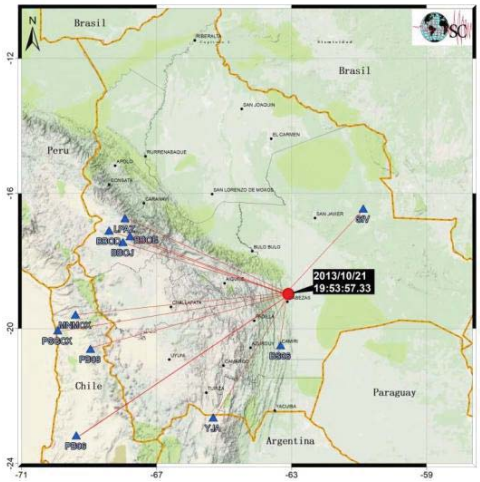

Figure 13. (a) Seismic event with a 61km error ellipse recorded on 2013–10–21 19:53:57.4. (b) Station distribution is not the best for this case, so depth and location uncertainty is high for this event.

(a)

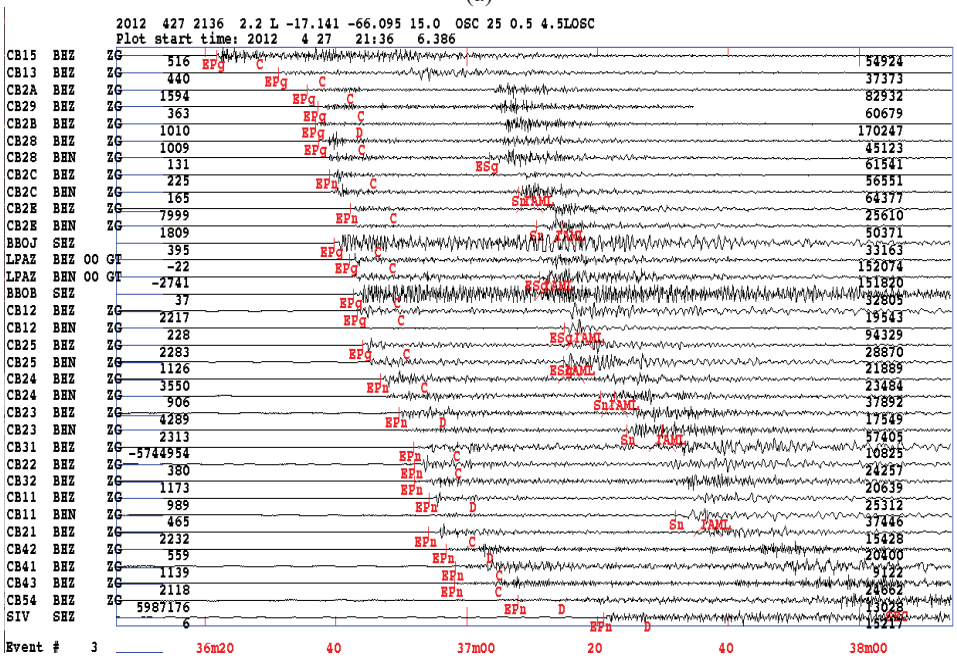

(b)

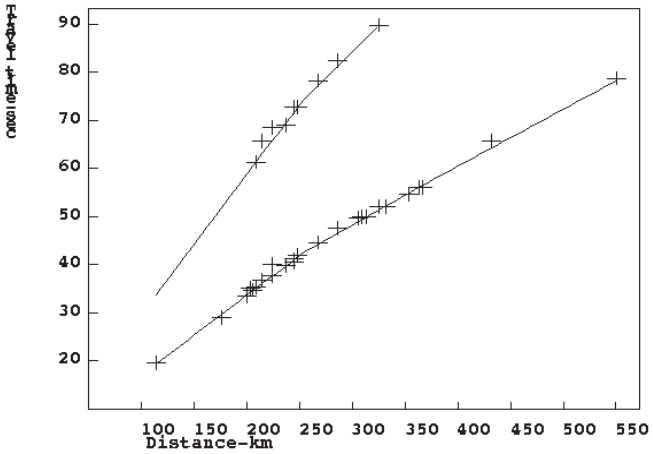

Figure 14. (a) Shallow Crustal seismic event, recorded on 27–04–2012 at 21:36:02.2 (UT) at Oruro, a depth of 25km and 4.5Mw magnitude. (b) Travel Times Curves fitted with seismic picks after the relocating, the lower line is for P and upper for S. *The cross represents picks done by iLOC and reviewed by analysts.*

4.2. Relative Location and Cross Correlation Technique

Once the proposed data list was reviewed manually and correlated with 3D software for location, we decided to perform one other procedure to optimize an almost absolute location to try and fit our data inside the GTx events.

Relative location is another technique that works effectively with aftershocks that are assumed to be near to the main shock. We applied it to certain earthquakes on the list

because they had data after the main seismic event. Diechman N. & Garcia-Fernandez M. (1992) said that aftershocks on a seismic cluster can be applied to obtain a better knowledge of the fault plane. They based their theory on the Cross – Correlation technique with a least – squares adjustment procedure.

The Cross – Correlation technique can resolve differences in hypocenter locations. Choosing a master event is the first step to compare other seismic events that may be located near the epicenter. Systematic errors resulting will likely be the same for all earthquakes near the hypocenter and, as a consequence, the final location will be minimally affected.

The basic principle of the algorithm used in the research is that a master event has its arrival times as compared with slave events. The waveform shape is also compared and then there is a shift on the slave event. There must be a fit for both waveforms. In other words, the picked phases of the slave event will be modified in order to retain just one reference time.

Along with the research and in order to improve and have more absolute earthquake locations, we applied this method to three important seismic events. First, Cabezas – Sta. Cruz Department on 2013, Lloja – La Paz Department on 2014 and San Martin – Oruro Department on 2016. A detailed procedure to perform a complete Cross – Correlation method is the paper presented by Gonzalo A. Fernandez et al. (2018), "Focal Mechanism of the 5.1Mw 2014 Lloja earthquake Bolivia: Probing the transition between extensional stresses of the central Altiplano and compressional stresses of Sub Andes".

Moreover, the earthquake of San Martin was also analyzed in this manner. The next figures show that when a seismic cluster is registered on a local and regional seismic network, all waveforms are quite similar.

(a)

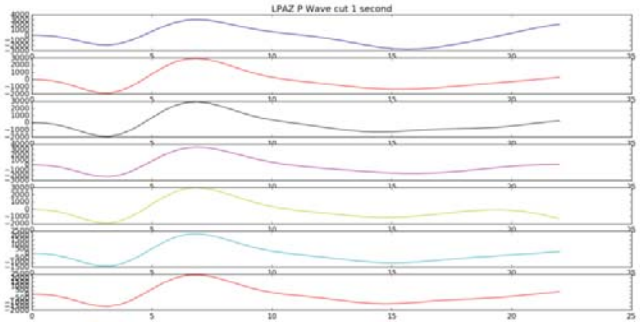

(b)

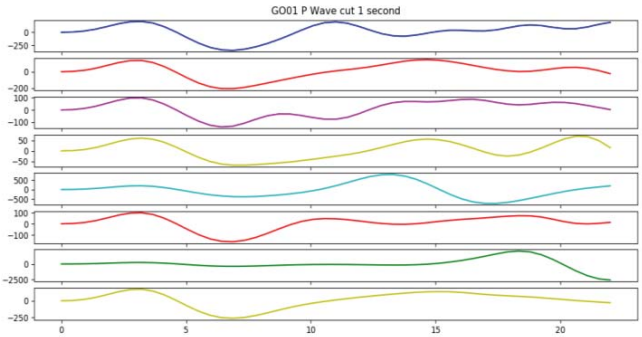

(c)

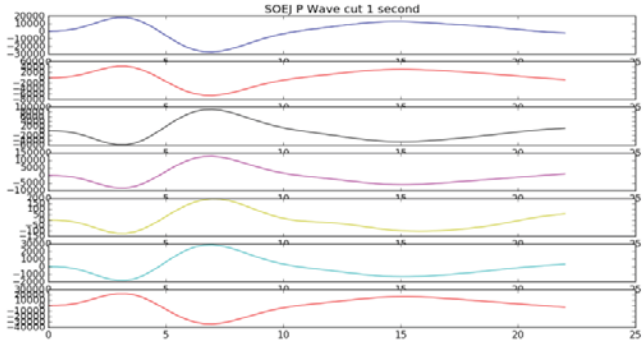

Figure 15. San Martin earthquake on 14-12-2016 at 19:23:43 UT. The first waveform is the master event, others are the slave events. (a) LPAZ station with all aftershocks of San Martin earthquake. (b) SOEJ station with all aftershocks of San Martin earthquake. (c) GO01station from Chile with all aftershocks of San Martin earthquake.

As mentioned before all waveforms display some similarity, even on the regional seismic stations such as GO01 from the Chilean network. After that, we applied the Cross-Correlation technique to associate each master event with slaves using a tool based on Obspy (Krischer et al. 2015) in order to get the best fit for each waveform.

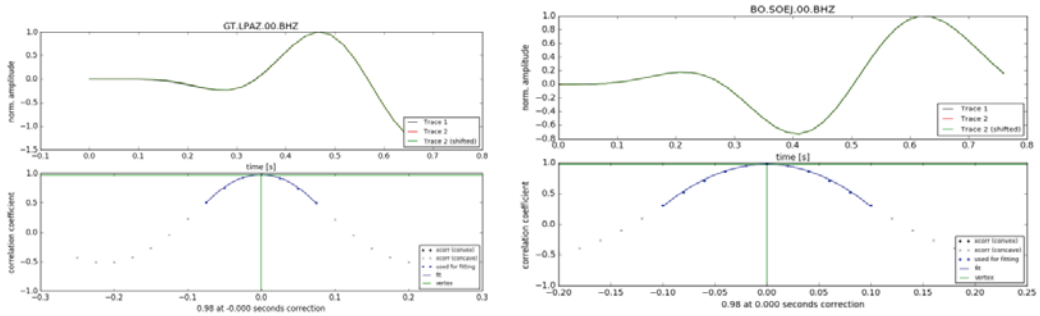

Figure 16. Correlating each waveform and channel in order to obtain a better fit using the algorithm from Diechman N. & Garcia-Fernandez M. (1992).

Finally, a plot showing the locations attempt and relative location was done. The original location, done with the JHD procedure is represented by green squares. The first refined location after the JHD and the 3D iloc software corrections are represented by red circles. We can show that there is an attempt of the events to realign. Black crosses represent the relative re-localization. The results show the crosses are aligned and can help to define the fault plane and tendency of a future mechanism

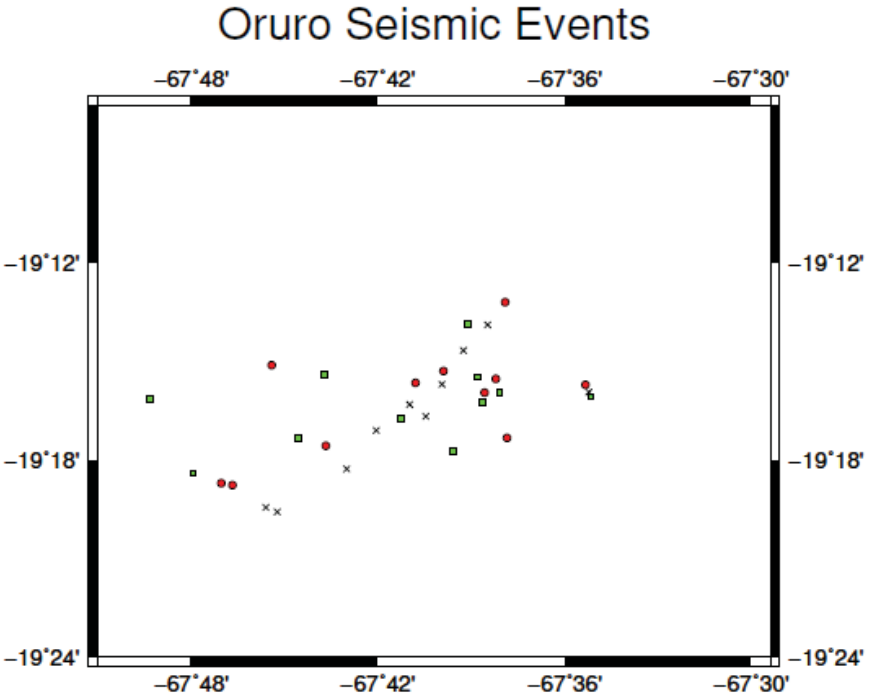

Figure 17. Seismic location of 2016-12-14 San Martin earthquake and aftershocks. *Red circles represent the first location. Green squares, the JHD and iLOC re localization and black crosses, the relative re localization using the Cross – Correlation technique.*

4.3. Focal Mechanisms and Moment Tensor Inversion analysis.

A focal mechanism is a geometrical or mathematical representation of the faulting during an earthquake. It is the representation of the relative motions of two blocks of Earth along a planar surface, referred to as a fault.

There are three angles that are important. The strike angle is the azimuth with respect to North of the trace of the fault on horizontal plane. The dip angle is the steepness of the fault, and the rake angle (also known as slip) is the direction of motion along the fault plane of the hanging wall relative to the foot wall.

A moment tensor is another description of the source mechanism of an earthquake. This requires that synthetic seismograms be represented as the linear combination of fundamental Green's function where the weights on these are the individual moment tensor elements (Jost and Herrmann 1989).

We applied the method proposed by Dreger et al. (2000). This method linearly inverts complete the three components of long or broadband seismograms from several local or regional distance stations to get the seismic moment tensor. There is no unique decomposition of the seismic moment tensor, but the one we will use is commonly employed during the routine analysis of some observatories in South America (Jost and Herrmann, 1989; Dreger et al., 2000).

It requires that the individual component moment tensors share the orientation of the principal eigenvector, which means it has a decomposition that includes double – couple, compensated linear vector dipole, and isotropic terms (Jost and Herrmann, 1989; Dreger et al., 2000).

The isotropic component is composed of three orthogonal force dipoles of equal strength with the same sign, the double couple is composed of two equal – strength, opposite – signed force dipoles that are oriented 45 degrees to the two orthogonal nodal planes (Dreger et al., 2000).

The CLVD is composed of three orthogonal vector dipoles. There is a major dipole, which has twice the strength of two opposite signed minor dipoles. It has been interpreted as a volume – compensated opening crack and has been argued to be a good model for spall (Dreger et al., 2000).

Later the basis Green's functions used during the analysis were computed using a frequency – wave number integration, Dreger et al. (2000) mention that this part of the code allows one to get more realist Green's functions based on the velocity model suggest by the user. In our case we apply Ryan's model presented in previous reports.

As we need to have a goodness of fit, we use Dreger et al.'s (2000) proposal to calculate the variance, which is computed as follows:

$$\sigma = \sum_i \sum_j \sum_k \frac{(d_{ijk} - s_{ijk})^2}{(N-M)} \quad (6)$$

where i, j, k, are the station, component and time sample, respectively, d and s are the observed and estimated time series, N is the total number of data points and M is the total number of free parameters.

Then we need to have a fit which is normalized by data power to yield a percent variance reduction, it is computed as follows:

$$VR = \left[1 - \frac{\sum_i \sum_j \sum_k (d_{ijk} - s_{ijk})^2}{\sum_i \sum_j \sum_k d_{ijk}^2}\right] * 100 \quad (7)$$

The variance is the quality control for the inversion. It is divided into stages that we briefly describe. From 0 to 20 represents a bad fit with no quality, from 20 to 40 represents a bad quality fit, from 40 to 60 represents a good fit of data, from 60 to 80 there is a good fit and data are coherent with good azimuthal coverage, then from 80 to 100 means that the solution is accurate and results are coherent.

Before this project, national researchers such as Cabre R. S.J., Drake L. S.J., Vega A., Ayala R. studied the Central Andes stress through focal mechanisms. At that time, earthquakes with magnitudes above 4.5 mb were studied, and the first P wave polarities were applied to determine the solution.

International agencies such as Global Centroid Moment Tensor (GCMT) also published the solutions for earthquakes that were registered with regional seismic stations. All proposed solutions are calculated by Moment Tensor Inversion technique.

Table 5. GCMT catalog for focal mechanisms in Bolivia.

Date and Time	Lat	Lon	Depth (Km)	Magnitude (mb)	Str	Dp	Rk	Source
1985-03-1910:28:46	-18.6	-63.700	42,0	5,5	136	40	74	GCMT
1985-03-2214:02:41	-18,6	-63.600	39,0	5,5	128	50	65	GCMT
1986-05-0916:23:59	-17,1	-65,600	13,0	5,6	108	64	29	GCMT
1986-06-1921:57:33	-17,0	-65.600	15,0	5,4	110	45	25	GCMT
1989-03-1617:12:21	-16,86	-64.930	35,4	5,1	171	9	127	GCMT
1998-03-01 01:51:04	-18,20	-65,40	43,0	5.2	354	50	172	GCMT
1998-05-22 04:49:02	-17,60	-65,20	15,0	6,6	186	79	178	GCMT
1998-05-26 01:08:19	-17,80	-65,34	28,6	5,4	204	64	-168	GCMT
1998-05-29 11:23:54	-17,64	-65,34	35,2	5,4	84	81	2	GCMT
2001-07-04 12:09:09	-16,92	-65,42	15,0	6,1	88	23	44	GCMT
2009-10-17 00:06:50	-18,55	-63.42	12,0	4,9	170	42	66	GCMT

Table 5. (Continued) GCMT catalog for focal mechanism in Bolivia.

2013-10-15 20:13:22	-18,32	-63,19	63,0	5,2	189	41	120	GCMT
2014-10-01 02:08:38	-16,57	-67,31	24,0	5,1	201	71	-178	GCMT
2015-12-21 16:21:7	-17,96	-65,36	14,0	5,1	188	57	162	GCMT

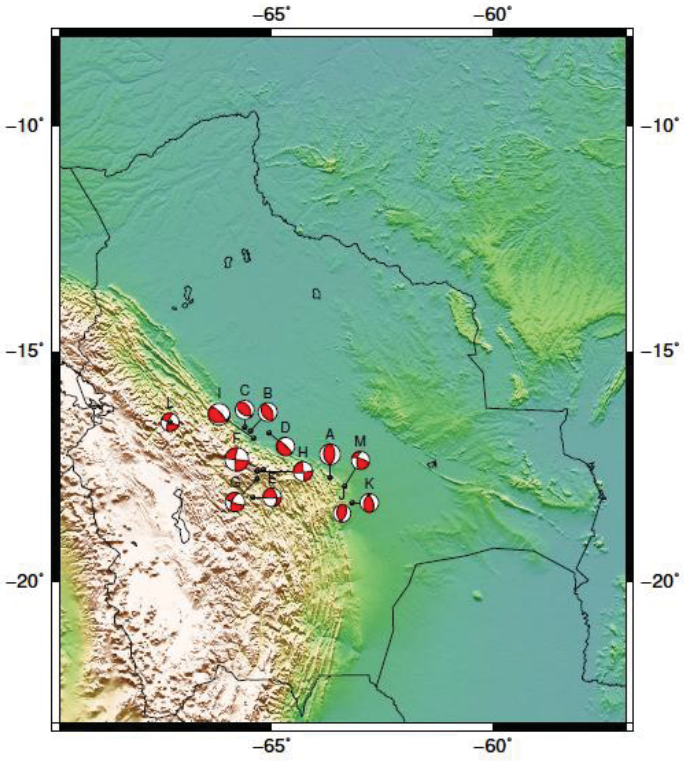

Figure 18. Focal Mechanisms through Moment Tensor Inversion computed by Global Centroid Moment Tensor (GCMT).

Table 6. Proposed solutions for focal mechanisms in Bolivia.

Date and Time	Lat	Lon	Depth (Km)	Magnitude (mb)	Str	Dp	Rk	Source
1968-08-08 00:06:42	-17.2	-64.800	72.0	4.9	105	69	158	Vega et al. 1991.
1969-07-18 23:17:09	-18.3	-63.3	8.0	5.5	139	41	17	Vega et al. 1991.
1972-05-12 17:16:20	-17.3	-66.2	43.0	5.0	97	53	152	Vega et al. 1991.
1976-02-22 08:09:23	-18.3	-65.3	41.0	5.2	117	61	151	Vega et al. 1991.
1981-07-23 13:51:26	-17.0	-64.9	38.0	5.3	103	66	163	Vega et al. 1991.
1985-03-19 10:28:46	-18.6	-63.7	42.0	5.5	136	39	104	Vega et al. 1991.
1985-03-22 14:02:41	-18.6	-63.6	39.0	5.5	347	46	117	Vega et al. 1991.
1986-05-09 16:23:59	-17.1	-65.6	13.0	5.6	106	64	157	Vega et al.

Table 6. (Continued) Proposed solutions for focal mechanism in Bolivia.

								1991.
1986-06-19 20:33:17	-17.0	-65.4	18.0	5.3	103	56	155	Vega et al. 1991.
1986-06-19 21:57:33	-17.0	-65.0	15.0	5.4	110	44	121	Vega et al. 1991.

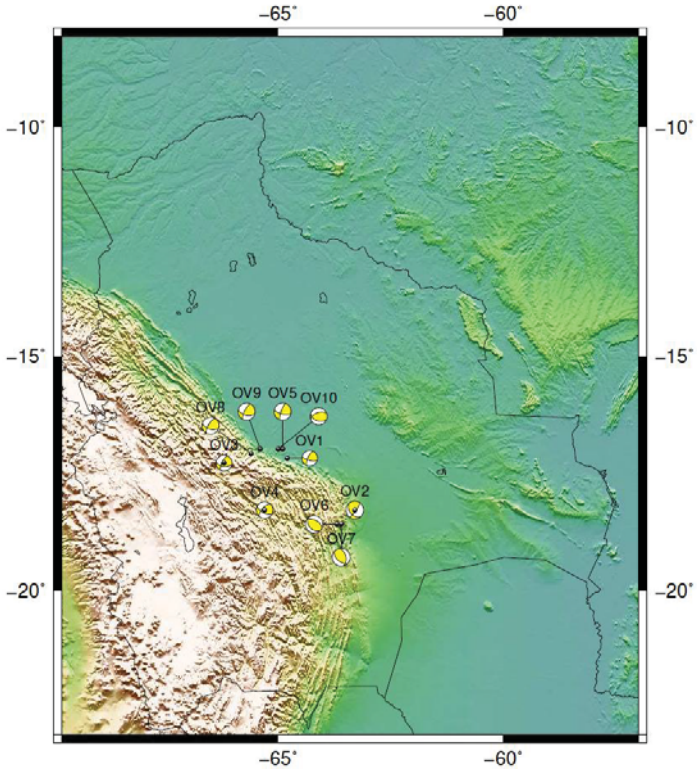

Figure 19. Focal Mechanisms through first P wave polarity solutions. *Vega and Burfon (1991) presented the solutions.*

Table 7. *Ayala and Vega (1999)* Proposed solutions for focal mechanisms in Bolivia.

Date and Time	Lat	Lon	Depth (Km)	Magnitude (mb)	Str	Dp	Rk	Source
1974-07-0116:51:00	-22.14	-64.74	17.0	5,5	168	29	90	RAS
1976-02-2208:09:23	-18,3	-65.300	41,0	5,2	117	61	32	VEGA-RAS
1969-07-1823:17:09	-18,3	-63.300	8,0	5,5	140	42	63	VEGA-RAS
1994-04-0309:01:04	-17,94	-64.990	10,0	5,3	267	67	43	RAS
1972-05-1217:16:20	-17,3	-66.200	43,0	5,0	99	54	26	VEGA-RAS
1968-08-2200:06:42	-17,2	-64.800	72,0	4,9	105	69	22	RAS
1981-07-2313:51:26	-17,0	-64.900	38,0	5,3	102	66	25	VEGA-RAS

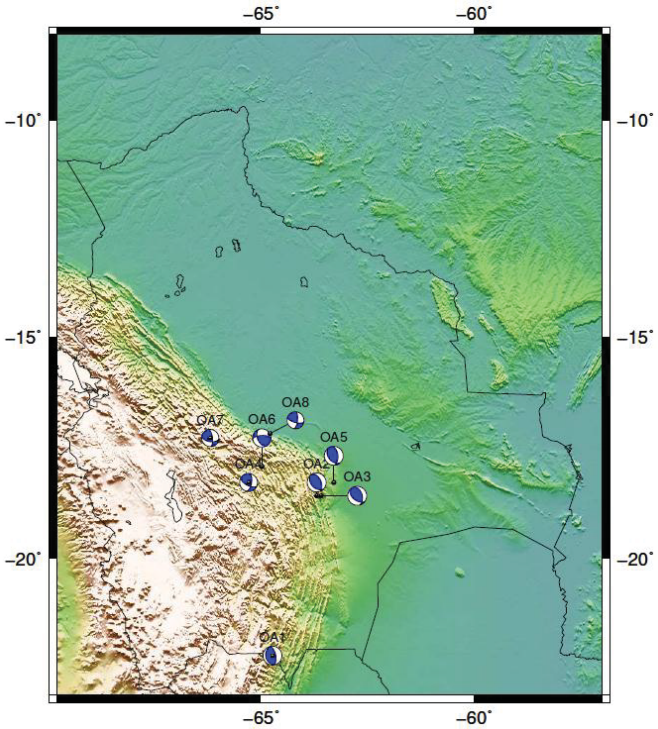

Figure 20. Focal Mechanisms through first P wave polarity solutions. *Ayala and Vega (1999) presented the solutions.*

We have selected a set of earthquakes after relocating and verifying the location parameters. The initial list was refined and now we present it as input for Focal Mechanisms or Moment Tensor Inversions. The following list was determined after all previous procedures related to localization from 2011 to 2015.

Table 8. Final earthquake list for Focal Mechanisms or Moment Tensor Inversions.

Date	Time	Lon	Lat	Depth (km)	RMS	Mag (Mw)	Strike	Dip	Rake	GT's ID
27/04/2012	21:36:04,01	-66,097	-17,14	14,2	0,58	4,5	179	76	-74	FS1
06/05/2012	17:09:50,16	-67,139	-17,904	7,4	0,55	4,6	264	20	0	FS2
26/06/2012	07:35:35,86	-66,09	-17,192	10,5	0,8	3,5	197	61	-41	FS3
15/04/2013	07:21:41,91	-65,436	-17,059	11,7	0,94	3,5	66	35	42	FS4
15/10/2013	21:59:32,98	-63,299	-18,444	10.0f	1,07	5,5	198	41	120	FS5
21/10/2013	19:53:57,33	-63,291	-18,52	45,1	0,68	4,1	0	51	90	FS6
01/10/2014	06:32:18,37	-67,068	-16,562	10.0f	1,19	5,1	294	44	-21	FS7
22/04/2015	21:08:40,00	-65,962	-17,236	32,8	0.44	4,5	143	56	-22	FS8

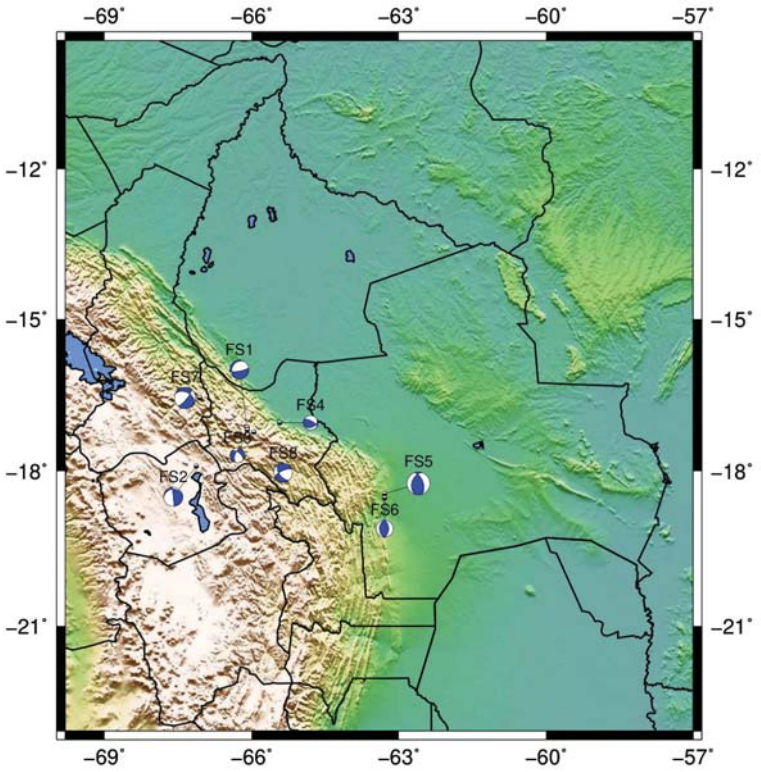

Figure 21. Focal Mechanisms solution proposed for the research project. *Eight solutions are plotted based on first polarity method, half of them are on the Bolivian Orocline, where the stresses shows a clear deformation and shortening for the Eastern Cordillera.*

- *FS – 1 / 2012 – 04 – 27 21:36:04.1 UT:*

This earthquake was located in the Central part of Bolivia, in Cochabamba. The nearest town is Chapisirca, where the local and CAUGHT seismic stations recorded the earthquake. The filter applied was from 0.05 to 0.08, which helped us to see the data quality while they were rotated. We used eight seismic stations out of twenty nine to try the inversion because the data quality was not the best.

Once the data were rotated and converted to displacement we were able to perform the inversion, according to Dreger et al.'s (2000) procedure. The first solution presented was computed by the FOCMEC method (Snoke et al., 2003), the main focal mechanism proposed on previous reports was a normal fault solution, at least 50% coherent with the geological context, however one plane was ambiguous (figure 22a).

The moment tensor inversion showed the synthetic waveform fitted with the data, which indicates a coherent solution, however the variance is about 40 to 60, which according to Dreger et al. (2000) means it has a quality of "2/4". The reason may be that all the data comes from the occidental side from Bolivia (OSC and CAUGHT seismic station located in the Altiplano and Western Cordillera).

We were not able to use SIV – AS008 data because of the velocity model which is not stable for the Sud Andes and Craton region. Figure 22 shows the result with strike, dip and rake information, Figure 22c show the results as moment tensor variables.

The preferred solution for this seismic event, is based on Dreger et al.'s (2002) method (figure 23a and 23b), because the data fit for the Transversal components showed consistency and the regional geological context shows the tendency of strike – slip faults over the place named before.

Table 9. Results from the Moment Tensor Inversion.

M0	2.545 e+22
Mw	4.2
% dc	60
% clvd	40
Strike / Dip / Rake	336; 68 / 84; 71 / -19;-173
Moment Tensor Variables	-0.57; 1.98; -1.40; 0.26; 1.72; 0.70

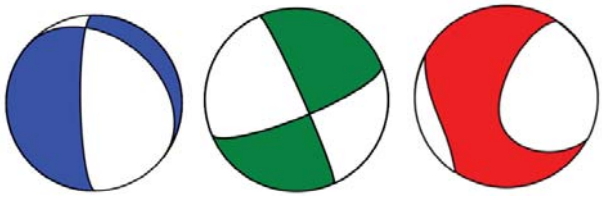

(a) (b) (c)

Figure 22. Proposed solutions for the seismic event of 2012-04-27 – GT1. (a) is the first proposed focal mechanism based on polarities of P waves with the FOCMEC method, (b) is the moment tensor solution based on Dreger's method, it changed to a srike – slip solution that is much more coherent than the first solution, and (c) is the same moment tensor solution as (b) but in terms of M.

(a)

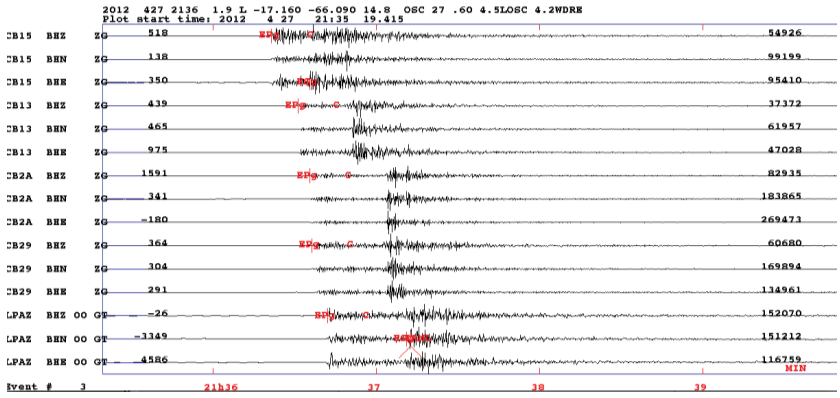

Figure 23. (a) The original data selected to do the inversion. (b) Data from the seismic event with coherent fit between synthetic and real data.
Red traces are the synthetics, black traces is the data rotated, filtered in displacement.

(b)

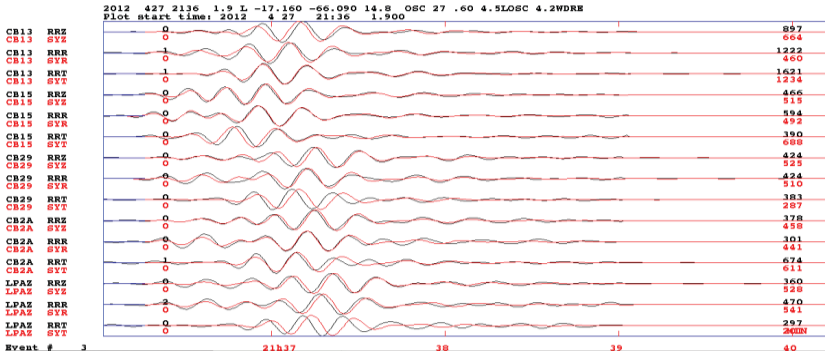

Figure 23. (Continued) (a) The original data selected to do the inversion. (b) Data from the seismic event with coherent fit between synthetic and real data.
Red traces are the synthetics, black traces is the data rotated, filtered in displacement.

- *FS – 2 / 2012 – 05 – 06 17:09:50.6 UT:*

Located in the Occidental part of Bolivia over the Altiplano, the nearest town to this event is Oruro, local, permanent, and also CAUGHT seismic stations recorded the earthquake. The filter applied was from 0.05 to 0.08, which helped us to see the data quality while they were rotated. We again used eight seismic stations out of twenty nine to try the inversion because the data quality was not the best.

Once the data were rotated and converted to displacement we were able to perform the inversion, according to Dreger et al.'s (2000) procedure, the first solution presented was computed by the FOCMEC method (Snoke et al., 2003). The main focal mechanism proposed on previous reports was a thrust fault solution, at least 45% coherent with the geological context.

According Dreger et al. (2000) it has a quality of "2/4". The reason may again be that all the data comes from the occidental side from Bolivia (OSC, IPOC - Chile and CAUGHT seismic station located in the Altiplano and Western Cordillera). Figure 24 shows the result with strike, dip and rake information, Figure 25a shows the results as moment tensor variables, also the Green's function fit are shown on figure 25b.

The preferred solution for this seismic event is based on Dreger et al.'s (2002) method (figure 25a and 25b). The data fit for the Transversal components showed consistency and the regional geological context shows the tendency of strike – slip faults, this time both planes were coherent with geological context.

Table 10. Results from the Moment Tensor Inversion.

M0	1.241 e+23
Mw	4.7
% dc	51
% clvd	49
Strike / Dip / Rake	165; 73 / 84; 78 / 12; 174
Moment Tensor Variables	-0.26; 0.76; -0.49; 0.30; 1.01; 0.22

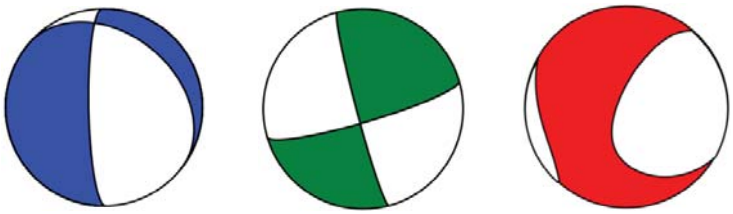

(a) (b) (c)

Figure 24. Proposed solutions for the seismic event of 2012-05-06 – GT2. (a) Is the first proposed focal mechanism based on polarities of P wave using the FOCMEC method, (b) is the moment tensor solution based on Dreger's method, it changed to a strike – slip solution which is coherent than the first solution, and (c) is the same moment tensor solution as (b) but in terms of M.

(a)

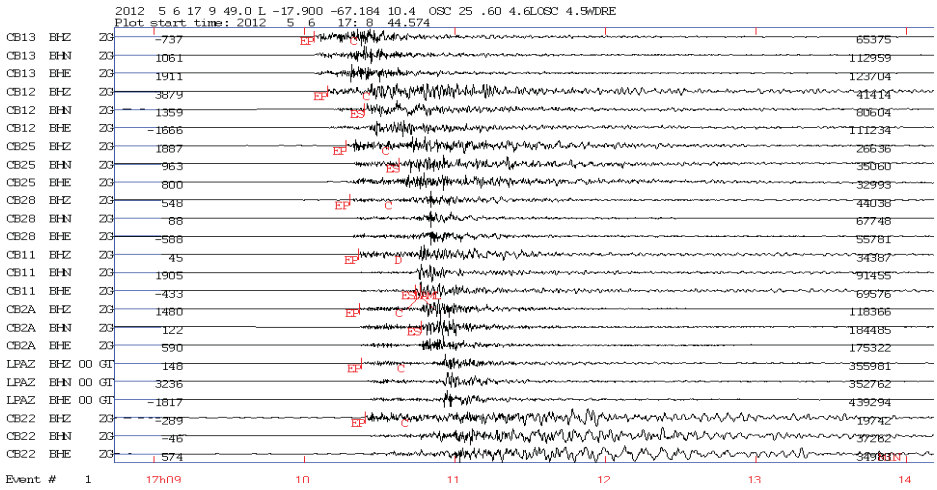

Figure 25. (a) The original data selected to do the inversion (b) Data from the seismic event with coherent fit between synthetic and real data

Red traces are the synthetics, black traces is the data rotated, filtered in displacement.

(b)

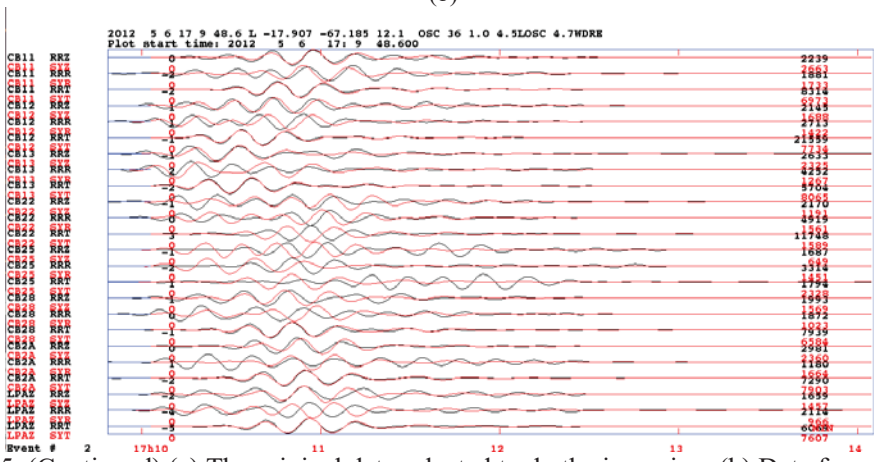

Figure 25. (Continued) (a) The original data selected to do the inversion. (b) Data from the seismic event with coherent fit between synthetic and real data.
Red traces are the synthetics, black traces is the data rotated, filtered in displacement.

- *FS – 3 / 2012 – 06 – 26 07:35:34 UT:*

This seismic event was located in central Bolivia, almost same region that FS – 1, however it was recorded by only a few seismic stations, again the OSC and CAUGHT project had the data.

It is well know that good azimuthal coverage for seismic events below 3.8 Mw is needed, if there are no enough seismic stations then a solution will not be the best while performing the moment tensor inversion. Unfortunately this seismic event does not have good azimuthal covertage due to lack of seismic stations.
We tried to apply a filter from 0.03 to 0.1 Hz but the data showed many oscillations and the seismic phases were not clear, then we applied a filter from 0.3 to 0.7 Hz and the data showed some consistency as displacement, however the quantity of stations decreased.

When we calculated the Green's function we found that there is not a good fit between the synthetic seismograms and the real data, Unfortunately we will not able to perform a moment tensor inversion due to the lack of data. Despite the attempts, the zoomed in view of synthetic and real data shows no consistency. Figure 26a shows the original data and figure 26b shows the synthetics in a shorter window.

(a)

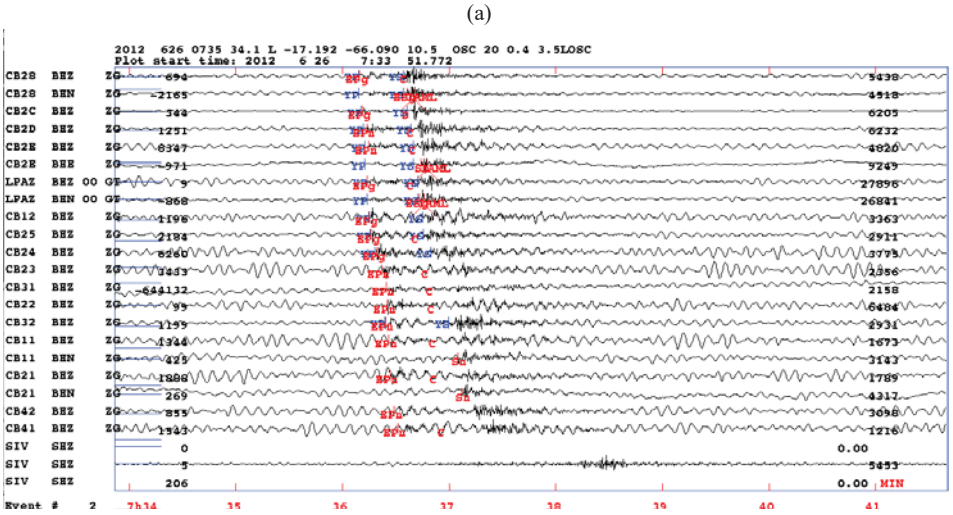

(b)

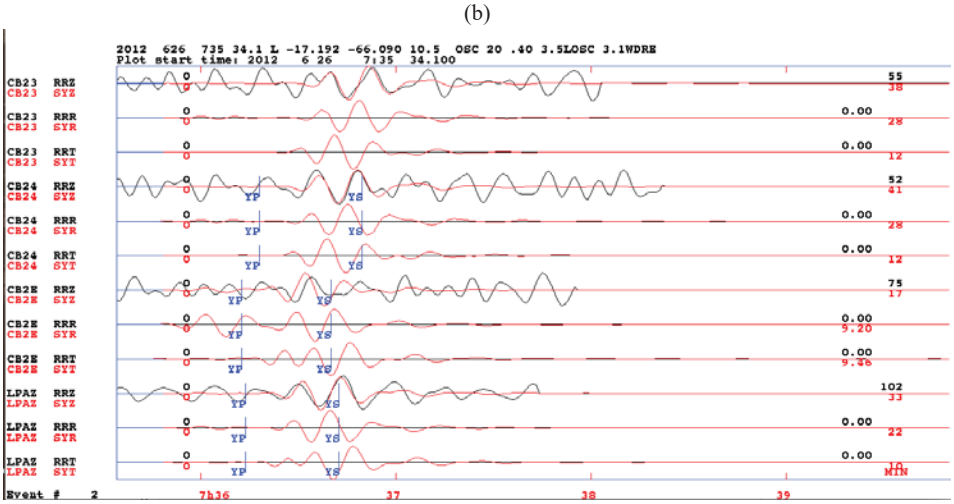

Figure 26. (a) The original data selected to do the inversion. (b) Data from the seismic event with no coherent fit between synthetic and real data. *Red traces are the synthetics, black traces is the data rotated, filtered in displacement but at the end of the data were cut.*

- *FS – 4 / 2013 – 04 – 15 07:21:39 UT:*

This seismic event is located at the Sud Andes region (Oriental side of Bolivia), the seismic station resolution is not the best due to the end of CAUGHT project, we only had the OSC's seismic network in the Altiplano . We added data from IPOC – Chile but there were no clear data, the seismic event magnitude is 3.5Mw, so not so many seismic networks recorded the earthquake.

The behavior of the data will be the same as FS – 3, so then we propose to keep the focal mechanism solution because at least one plane is coherent with geological data. Please refer to Table 1 for more information.

- *FS – 5 / 2013 – 10 – 15 21:59:32 UT and FS – 6 2013 – 10 – 21 19:53:57.7 UT:*

This seismic event was studied with the University of Sao Paulo coordinating and getting the focal mechanism solution based on P wave polarities. The solution is consistent with the geological context. Moreover the cross correlation technique let us determine the absolute relocation of the seismic event using the body waves.

Again the lack of seismic station coverage would not let us perform a seismic moment inversion, however the good azimuthal coverage of three seismic stations has let us determine the focal mechanism solution and the stress drop. Moreover we determined that the Mandeyapecua fault is not the main source of the seismic event.

Figure 27 shows the relocation result and the focal mechanism, which is better than our solution. The plots show a strike of 198, dip of 41 and rake of 120 degrees, the coherence of the LPAZ data after applying the cross correlation method, and a map with the seismic stations that we applied during the cross correlation.

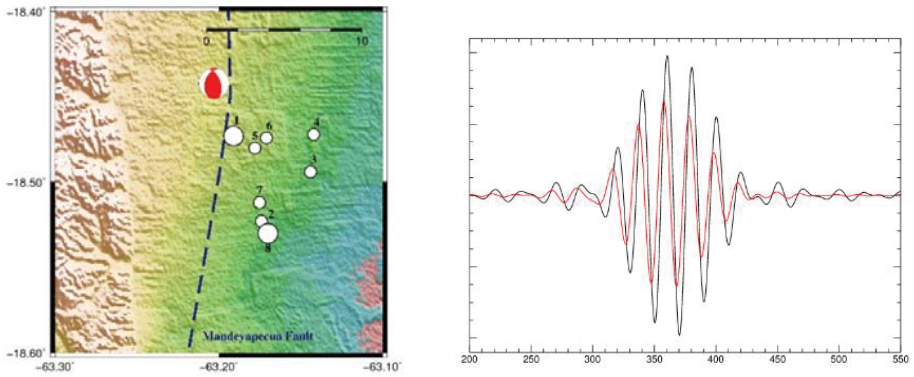

Figure 27. (a) Focal mechanism solution based on the relative location based on the cross correlation method, (b) LPAZ data with good fit between the main shock and aftershocks, and (c) stations that were included during the analysis.

- *FS – 7 / 2014 – 10 – 01 06:08:32 UT:*

This seismic event was located in the transition between the Central Andes and the Sub Andes Bolivian region. We developed an independent approach that involved cross correlation to do the relative relocation, then focal mechanism and moment tensor inversion. We did all the procedures separately because the seismic event was strongly felt all over La Paz city. For more details on the results please refer to "Focal mechanism of the 5.1Mw 2014 Lloja earthquake, Bolivia: Probing the transition between extensional stresses of the central Altiplano and compressional stresses of the sub – Andes" https://doi.org/10.1016/j.jsames.2019.01.001.

The figure 28 shows the result of the relocation (same as proposed during all the previous reports), also the focal mechanism solution compared with international agencies. Our solution is the most coherent with the geological context and with the inversion that is shown in figure 28.

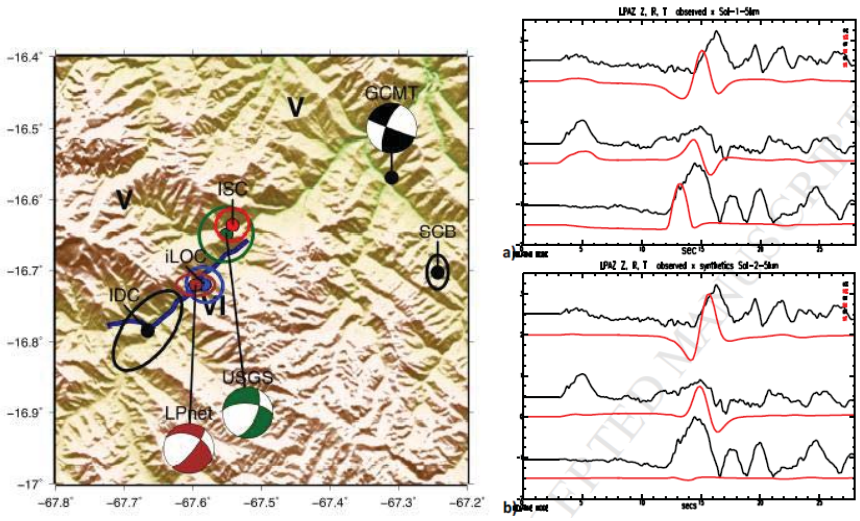

(a) (b)

Figure 28. (a) Focal mechanism solution based on the relative location based on cross correlation method and FOCMEC software, and (b) LPAZ data with good fit between the synthetics and real data.

- *FS – 8 / 2015 – 04 – 22 21:08:40.6 UT:*

The seismic event was located in the central part of Bolivia, in the Eastern Cordillera, near the Cochabamba department. In this region it is very common to have shallow crustal earthquakes, however as there are not any seismic stations nearby, again the azimuthal coverage is not the best.

Despite this problem, we were able to record clear polarities of the P wave from the stations. The solution proposed is a strike – slip mechanism, the plane which is coherent, geologically speaking, has 143, 43, -22 as the strike, dip and rake. As we mentioned before we prefer to keep this seismic event with a focal mechanism solution to help us to understand the fault behavior over the region.

5. CONCLUSIONS

The Central Andes is composed of five morpho-tectonic units (Western Cordillera, Altiplano, Eastern Cordillera, Inter Andes, Sub Andes). The Chaco – Beni Basin is a good example of the continuous compression and extension process due to the subduction between Nazca and South America plates.

Despite the efforts made in previous research, a well constrained velocity model was not available for the Central Andes, so there is seismic location uncertainty for shallow crustal earthquakes

The crustal thickness studies conducted in the Central Andes developed by Ryan et al. (2016) and Ward et al. (2013) have made it feasible to elaborate a 1D velocity model for the Western Cordillera, Altiplano and Eastern Cordillera. Unfortunately the lack of seismic stations does not allow for complete coverage of the Inter Andes and Sub Andes.

The earthquake location algorithms such as Joint Hypocenter Determination, VELEST. iLOC (Bondar and Storchak, 2011) have helped refine the initial velocity model. Further, the list of earthquakes presented at the beginning of the report were extensively analyzed using the algorithms mentioned. A coherent and accurate list of earthquakes has been produced after all relocations, and eight candidates are presented to calculate the fault plane solution or moment tensor.

The relative location procedure using the cross correlation technique (Diechmann N- & Garcia-Fernandez M. 1992) was used for some earthquakes that had aftershocks. Their alignment has let us assume a possible fault plane. Cabezas 2013 at Santa Cruz, Lloja 2014 at La Paz, and San Martin 2016 were the earthquakes that have been analyzed with the mentioned technique.

The quality control over the waveform and the location parameters provided us accurate information for beginning the procedure to calculate focal mechanisms through first P wave polarities. FOCMEC (Snoke 2003) was the algorithm that was used. A grid search method of 15 ° was set up in order to look for the best solutions.

There are however some ambiguities in the solutions that are located in the Inter Andes and Sub Andes regions due to the poorly constrained 1D velocity model. To try to reduce this issue, we fixed the depth and we increased the grid search to 25° for the earthquakes that were from Cordillera region in the Sub Andes.

From the proposed list only three earthquakes were able to be modeled by Moment Tensor Inversion (Dreger et al., 2000), the FS1 – Cochabamba 2012, FS2 – Oruro 2012 and FS7 – Lloja 2014, showed coherent results and acceptance criteria (VR) of 2/4.

A filter band in displacement of 0.05 to 0.08 Hz was used, the Greens' Functions fit with no problem, and a grid search of 5° was computed. From the results of the moment tensor inversion we were able to obtain the strike, dip and rake angles to plot the focal mechanism.

As described, in theory the velocity model plays an important role during the procedure. The earthquakes that presented coherent results are located in the Altiplano and Eastern Cordillera. Other earthquakes were located in the Inter Andes and Sub Andes. For that reason the Greens' Function did not fit at all over the displacement waveforms.

However the focal mechanism solutions presented are coherent in one plane. The plane was correlated with geological information and with the solutions presented by GCMT. Further the improvement in our locations helped us to define better the local hazard.

After almost 15 years an accurate velocity model in 1D for routine use is presented and evaluated with positive results, and the first three moment tensor solutions are saved in our national data base to enhance knowledge of seismicity. Moreover they will be proposed to be part of GCMT catalog.

REFERENCES

Beck, S. L. and G. Zandt, 2002, Nature of orogenic crust in the central Andes, J. Geophys. Res., 107, No. B10, p. 2230.

Beck, S. L., G. Zandt, S. Myers, T. C. Wallace, P. Silver, and L. Drake, 1996, Crustal thickness variation in the Central Andes, Geology, 24, pp. 407-410.

Bondár, I. and D. Storchak, 2011, Improved location procedures at the International Seismological Centre, Geophys. J. Int., 186, pp. 1220-1244.

Bondár, I. and K. McLaughlin, 2009, Seismic location bias and uncertainty in the presence of correlated and non-Gaussian travel-time errors, Bull. Seism. Soc. Am., 99, pp. 172-193.

Deichman, N. and Fernandez M. G., 1992, Rupture geometry from high-precision relative hypocentre locations of micro earthquake clusters, Geophys. J. Int., 110, 3, pp. 501-517.

Dreger, D., H. Tkalcic, and M. Johnston, 2000, Dilational processes accompanying earthquakes in the Long Valley Caldera, Science, Vol. 288.

Dreger, D. and B. Woods, 2002, Regional distance seismic moment tensors of nuclear explosions, Technophysics, 356, pp. 13-156.

Eichelberger, E., N. McQuarrie, J. Ryan, B. Karimi, S. Beck, and G. Zandt, 2015, Evolution of crustal thickening in the central Andes, Bolivia, Earth and Planetary Science Letter, 426, pp. 191-203.

Jost, M. L. and Herrmann, 1989, A student guide to and review Moment Tensor, Seismological Research Letter, Volume 60, No. 2.

Lienert, R. and J. Havkov, 1995, A Computer Program for Locating Earthquakes Both Locally and Globally, Seismological Research Letters Volume 66, Number 5, September-October 1995.

Minson , S. and D. Dreger, 2008, Stable full moment tensor inversions, Geophys. J. Int., 174, pp. 585-592.

Myers, S., S. Beck, G. Zandt, and T. Wallace, 1998, Lithospheric-scale structure across the Central Andes of Bolivia from seismic velocity and attenuation tomography, J. Geophys. Res., 103, pp. 21,233-21,252.

Myers, S. C., M. L. Begnaud, S. Ballard, M. E. Pasyanos, W. S. Phillips, A. L. Ramirez, M. S. Antolik, K. D. Hutcheson, J. J. Dwyer, C. A. Rowe, and G. S. Wagner, 2010, A crust and upper-mantle model of Eurasia and North Africa for Pn travel-time calculation, Bull. Seism. Soc. Am., 100, pp. 640-656.

Ryan, J., S. Beck, G. Zandt, L. Wagner, E. Minaya, and H. Tavera, 2016, Central Andean crustal structure from receiver function analysis, Tectonophysics, 682, pp. 120-133.

Snoke, A, 2003, FOCMEC, Focal Mechanisim Solution, http://www.geol.vt.edu/outreach/vtso/focmec/.

Ward, Kevin M., Ryan Porter, George Zandt, Susan Beck, Lara Wagner, Estela Minaya, and Hernando Tavera, 2013, Ambient Noise Tomography Across the Central Andes, Geophys. J., https://doi.org/10.1093/gji/ggt166.

LIST OF SYMBOLS, ABBREVIATIONS, AND ACRONYMS

AFRL	Air Force Research Laboratory
AFSPC	Air Force Space Command
AFWA	Air Force Weather Agency
ISC	International Seismological Center
OSC	Observatorio San Calixto
MTI	Moment Tensor Inversion.

DISTRIBUTION LIST

DTIC/OCP
8725 John J. Kingman Rd, Suite 0944
Ft Belvoir, VA 22060-6218 1 cy

AFRL/RVIL
Kirtland AFB, NM 87117-5776 1 cy

Official Record Copy
AFRL/RVB/Dr. Frederick Schult 1 cy

This page is intentionally left blank.